学位論文

Unconscious neural mechanism involved in access processing to visual awareness (視覚的意識へのアクセス処理に関与する無意識下の神経メカニズム)

2023 年 3 月

栗田 佑騎

CONTENTS

3. Experiment 1: Correlation between vMMN and APVA

4. Experiment 2: The role of mismatch process in AVPA

5. Experiment 3: Effect of change-related response on APVA

1. Introduction

Is what we “see” really everything that is in front of us? Despite the scene in front of us is transmitted through the retina and that visual information is input into the brain, there are some things that we can consciously perceive (“seen”) and others that we cannot (“unseen”). For example, you should have seen all the text in front of you, but you can perceive and read only a small part of it. In fact, most of human information processing is done unconsciously, and we see “the world” after the unconscious information processing. However, previous studies related to consciousness aim to clarify ‘where in the brain the conscious experience occurs’, and unconscious neural processing has not been much examined. I believe it is important to clarify the unconscious neural processing in order to better understand the human visual cognitive systems. In this study, we hypothesize a certain unconscious neural processing, and clarify the neural mechanism underlying that processing from the viewpoint of electroencephalograms.

Many previous neuropsychological studies on visual awareness have been trying to elucidate neural processes that are correlated with the subjective conscious experience, analyzing the differences in neural activities between when the visual stimulus is consciously perceived and when it is not (Koivisto & Revonsuo, 2010; Dehaene & Changeux, 2011; Aru et al., 2012; Silverstein et al., 2015; Koch et al., 2016). Studies of the neural correlate of consciousness (NCC) using functional magnetic resonance imaging (fMRI), which has high spacial resolution and the temporal resolution on the second timescale, indicated that the posterior cortical areas are related to the neural mechanism of visual awareness (e.g., Lumer et al., 1998; Polonsky et al., 2000; Lee et al., 2005; Frässle et al., 2014). On the other hand, studies using electroencephalography

(EEG) focusing on the temporal aspect of NCC on the millisecond timescale, indicated that visual awareness negativity (VAN) was observed at a latency of about 200 ms after visual stimulus onset when the visual stimulus was consciously perceived (For review: Koivisto & Revonsuo, 2010; Förster et al., 2020). VAN is one of the earliest brain activities related to visual awareness and is often used as an index of visual awareness (Koivisto & Revonsuo, 2003; Koivisto et al., 2009; Koivisto & Revonsuo, 2010; Pitts et al., 2014; Eklund & Wiens, 2018). From the viewpoint of whether VAN is related to the conscious or unconscious processing, some studies reported that VAN does not reflect unconscious neural processing, rather it presents the stage of graded visual consciousness (Koivisto & Grassini, 2016; Koivisto et al., 2017). However, neural activity related to unconscious information processing has not been clarified yet.

We hypothesized that a type of the unconscious neural processing that determines whether the unconscious stimulus is consciously perceived or not (Hereafter, access processing to visual awareness (APVA)) at the earlier stage of visual processing than the emergence of VAN. Attention is considered to be necessary for conscious experience or perception of visual stimulus (Prinz, 2011; Bor & Seth, 2012; Cohen et al., 2012). According to these previous studies, attentional mechanisms would impinge on visual processing earlier than the emergence of VAN. These attentional mechanisms were considered to be restricted to those accompanied by visual processing earlier than VAN. Regarding whether attention is directed to unconscious stimuli, a previous study indicated that attention is directed to unconscious visual stimuli and that attention makes it easier for these to be perceived consciously (Jiang et al., 2006). An abruptly-presented visual stimulus, inducing attentional capture at a certain location of the visual field, was also reported to facilitate conscious perception of a subsequent in near-threshold target image at the location (Chica et al., 2010; Chica et al., 2011). Therefore, the attentional mechanism induced by the unconscious visual stimulus appears to facilitation of visual processing in response to the unconscious visual stimulus, so that the stimulus information crosses the boundary between consciousness and unconsciousness.

In the study of NCC, binocular rivalry has been a useful tool to distinguish between the conscious and unconscious neural process (Crick & Koch, 1990). Binocular rivalry is a phenomenon in which only one image is perceived when different visual images are presented to the right and left eyes, and the perception is automatically and alternatively switched. Perceptual alternation of bistable images is well known to be caused by sudden external stimulus changes such as flash (Kanai et al., 2005). In binocular rivalry, change-related responses have been reported to be involved in perceptual alternation (Veser et al., 2008; Roeber et al., 2008; Roeber et al., 2011). Change-related responses mean visual evoked potential (VEP) induced by a change of visual stimulus. Generally, P1 (the positive peak observed in occipital region at about 100 ms after the onset of visual stimulus) and N1(the negative peak observed in occipital region at about 130‐200 ms after the onset of visual stimulus) are typical neural activities of the change-related responses. According to these studies, early neural components at occipital and parietal sites are associated with hastening perceptual alternation on binocular rivalry. However, many studies on NCC focus on the static contrast of neural responses when images are consciously perceived or when they are not, and it has not been clarified yet what neural mechanisms cause dynamic processing related to conscious perception such as APVA (Salti et al., 2019).

If VAN is one of the earliest neural activity that reflects conscious experience, there must be the neural activity related to the unconscious processing at the stage before 200 ms when VAN occurs. We focused on visual mismatch negativity (vMMN) as one of the neural mechanisms involved in APVA. VMMN is a negative-going enhancement in VEP over posterior electrodes at a latency of approximately 130–250 ms when comparing responses to an infrequently presented visual stimulus (deviant) and a repetitively presented stimulus (standard) (Czigler et al., 2002; Astikainen et al., 2008; Kimura et al., 2009). This negative-going component appears even when participants does not pay attention to the deviant, and the negativity is interpreted to reflect automatic visual change detection based on temporal regularity. VMMN appeared when the deviant was unconsciously presented using binocular rivalry (Jack et al., 2017). In other words, vMMN, which is an earlier VEP component than VAN, originates from the unconscious neural mechanism. In addition, visual change detection is involved in the orienting response, which is the function of trying to reallocate attention to the novel stimulus before perceiving it, to the deviant (Astikainen et al., 2008; Urakawa et al., 2010). The attentional orienting response induced by the visual mismatch process to the unconscious deviant would be relevant to the conscious perception of the deviant stimulus. However, the relationship between vMMN and behavior, in addition to conscious perception, has not yet been well-established because vMMN is merely assumed to reflect automatic visual change detection (Stefanics et al.,2014). We hypothesized that vMMN evoked by the unconscious deviant is involved in APVA.

To clearly specify the processing of APVA driven by the mismatch, we further focused on visual mismatch oscillatory responses (vMORs), induced oscillatory responses of visual mismatch process. VMORs have been reported to be an enhancement of the oscillatory responses (e.g., spectral power, phase locking) in the theta band (4–8 Hz) over posterior electrodes at a latency of approximately 100–350 ms when comparing responses to the deviant and standard stimulus (Stothart et al., 2013; Yan et al., 2017). According to these studies, the enhancement of event-related spectral perturbation (ERSP) and inter-trial phase coherence (ITPC) in the theta band to the deviant stimulus has different roles in the neural mechanism of the visual mismatch process. On the other hand, recent studies of oscillatory NCC have reported that theta band activities in the posterior and frontal cortical areas are involved in conscious visual perception (Davidson et al., 2018; Drew et al., 2019; Haque et al., 2020). These studies suggest that the theta band activity is involved in the neural process of conscious perception. If the theta band activity is related to the neural process of conscious perception, vMORs in the theta band will also play an important role in APVA. Therefore, we hypothesized that vMORs in the theta band are also involved in the neural mechanisms of APVA as well as vMMN.

ERSP and ITPC in each frequency band are calculated by time-frequency analysis of EEG signals. Continuous wavelet transform is used for the time-frequency analysis. Continuous wavelet transform for EEG is a common method to extract the information of amplitude and phase for each frequency band from EEG time series at a certain timepoint. These amplitude and phase are calculated by setting the wavelet in each frequency band using the short wave which rapidly attenuates with time (Mother wavelet), and integrating them to EEG signals at each timepoint (Torrence & Compo, 1998; Ashmead, 2010; 開 & 金山, 2020). In the analysis of EEG, Morlet wavelet, which is considered to be close to biological signals, is often applied as Mother wavelet in the continuous wavelet transform. ERSP is calculated by summing the squared amplitudes. Generally, an enhancement of ERSP reflects an increase of neural activity. On the other hand, ITPC is calculated by averaging the unit vectors with phase over trials. ITPC has a magnitude from 0 to 1 and represents the degree of synchrony of EEG signals over trials. In general, it represents the amount of change in the rhythm of brain activity caused by a certain stimulus. Analyzing ERSP and ITPC enable us to focus on the frequency characteristics of brain activity that are difficult to capture only by analyzing VEP.

2. Purpose

The main goal of the present study is to clarify the neural mechanism of APVA, which has not been well-established so far in the field of visual awareness. To quantitatively evaluate APVA, we used the proportion of perceptual alternation on binocular rivalry. We then investigated the correlation between vMMN, vMORs, change-related response (N1) and the facilitation of perceptual alternation, respectively. Such an evaluation of the relationship between behavioral and neural data with a focus on inter-individual difference is a powerful analytical approach for induction of the neural mechanisms underlying behavioral data (Vogel and Awh., 2008). In order to clarify the relationship between these neural components and the facilitation of APVA, we executed three experiments as follows: Experiment 1, Experiment 2, and Experiment 3.

In Experiment 1, to clarify whether vMMN affects APVA, we conducted the modified oddball paradigm on binocular rivalry, based on previous studies (Jack et al., 2017; Urakawa et al., 2017a). Under this stimulation paradigm, we recorded vMMN and perceptual alternation from before to after the presentations of the standard and deviant stimulus in binocular rivalry. The proportion of perceptual alternation under the standard was subtracted from that under the deviant, so as to evaluate the facilitation of APVA by the deviant. In order to clarify the relationship between vMMN and APVA, we focused on inter-individual variability and then examined whether vMMN enhancement is correlated with an increase in the proportion of perceptual alternation across participants, as in the previous studies for the bistable image of Necker cube (Urakawa et al, 2017a; Urakawa et al, 2018).

The purpose of the Experiment 2 is to examine the relationship between theta band vMORs and APVA. To clarify whether vMORs in the theta band affect APVA, we further analyzed event-related spectral perturbation (ERSP) and inter-trial phase coherence (ITPC) in the theta band for EEG data in Experiment 1. We then investigated the inter-individual variability between ERSP/ITPC enhancement in the theta band and the proportion of perceptual alternations. The Experiment 2 is expected to clarify whether neural processing related to vMORs, which is little known so far, is involved in APVA, and if so, how it is related.

The perceptual alternation of binocular rivalry may occur by sudden stimulus changes without temporal regularity as described in the third paragraph. In other words, it is considered that a neural mechanism based on change-related responses is relevant to APVA. In order to test this hypothesis, we conducted the Experiment 3 in which sudden stimulus changes without temporal regularity were presented unconsciously. The purpose of the Experiment 3 is to examine whether change-related response (N1) is involved in APVA. The Experiment 3 will clarify whether the important neural mechanism involved in APVA is a vMMN-specific mechanism or a common mechanism between vMMN and change-related response.

3. Experiment 1: Correlation between vMMN and APVA

To clarify whether vMMN affects APVA, we examined the correlation between vMMN and the perceptual alternation in binocular rivalry. This chapter describes the experimental procedures, analysis methods, results, and discussions of Experiment 1. Contents of this chapter is also described in the published paper (Kurita et al., 2021).

3.1. Methods

3.1.1. Subjects

Nineteen healthy volunteers (19 males, age 21–36 years, mean ± SD, 23.2 ± 3.3 years) participated in this experiment. All the participants were right-handed and had normal or corrected-to-normal visual acuity. Informed consent was obtained from all participants, and this experiment was approved by the ethics committee of Tokyo University of Science.

3.1.2. Stimulus and Procedure

Figure 1 shows the stimuli and the stimulation procedure for one trial. Images were presented on a liquid crystal display (BenQ XL2540) using the MATLAB Psychophysics Toolbox (Brainard, 1997; Pelli, 1997). The participants were presented with two computer-generated images using a mirror stereoscope. The image included annulus-shaped gratings with a spatial frequency of 1.3 cycles/degree. The outer radius of the gratings was 4.3° and the inner radius was 0.57°. A white fixation point was presented at the center of the grating image. The blue or red grating was presented on a black background, with a mean luminance of 0.05 cd/m^2. The mean luminance of the red portion was 3.56 cd/m^2, whereas that of the blue portion was 2.16 cd/m^2. Each grating was surrounded by three white rings that served to lock the vergence. Each white ring had a line width of 0.19°. The outer radius of the largest ring was 8.64°, and the outer edges of each of the other two smaller rings were inwardly depicted by 0.64° from the outer edge of the neighboring larger ring. White rings in both eyes were continuously presented throughout the stimulation period.

Figure 1(a) shows the procedure of the stimulation for one trial. Based on a stimulation scheme used in the previous studies (Urakawa et al., 2017a; Urakawa et al., 2017b; Urakawa et al., 2018), each trial had two consecutive phases. In the first phase, an identical grating image was simultaneously presented to both the left and right eyes. The grating images were intermittently presented 23 times, with a duration and inter-stimulus interval (ISI) of 200 ms and 100 ms, respectively. The grating was either blue or red, and its orientation was either horizontal or vertical. Between these images, an image without grating was presented for 100 ms in both eyes. In the presentation of the grating image, the colors were counterbalanced across the trials for each participant. The orientation of the grating in the first phase was maintained constant for each participant, and then it was counterbalanced among the participants. In the first phase, participants were asked to look at the fixation point passively. Immediately following the first phase, in the second phase, the grating image was manipulated to induce binocular rivalry by changing its color from blue to red or vice versa for either eye at the beginning of the second phase. The color change was counterbalanced between the two eyes. Similar to the first phase, the gratings in the second phase were simultaneously and intermittently presented, without changing the grating image for each eye. The duration and ISI used in the second phase were the same as those used in the first phase. They were expected to mitigate binocular fusion

(Wolfe, 1983). According to the previous psychophysiological studies (e.g., Astikainen et al., 2008; Kimura et al., 2009; Urakawa et al., 2017a; Urakawa et al., 2018), vMMN was also expected to appear in the duration and ISI. In the intermittent stimulation of the second phase, the gratings were presented seven times. During the second phase, a white fixation cross appeared at the center of the grating image instead of the white fixation point. When the white cross appeared (i.e., when the second phase started), the participants were required to fixate on the cross and press a key on the keyboard in front of them to start reporting a perceived grating image. In this behavioral task, participants were asked to continuously press the left arrow key during the period in which blue grating was perceived, or to continuously press the right arrow key during the period in which red grating was perceived. Meanwhile, during the period in which blue and red gratings merged in perception, the participants were instructed not to press any key. This behavioral task was continued throughout the second phase. In every trial, participants were asked to maintain their initial perception during the second phase as much as possible. The second phase ended with a blank image that lasted for 100 ms, as in the first phase. Following the termination of the second phase, the target stimulus was immediately presented for 500 ms. The change in orientation (from horizontal to vertical or vice versa) corresponded to the deviant that violated the preceding sequential regularity, which was a repetition of an identical orientation from the beginning in the first phase. In this orientation manipulation, the colors of both eyes remained same. As illustrated in Figure 1(b), the target stimulus yielded three conditions dependent on the subject's conscious/unconscious percept just before itself: the standard (STD) condition, the unconscious-deviant (Uncon-DEV) condition, and the conscious-deviant (Con-DEV) condition. In the STD condition, the target stimulus was the same as the grating images used in the second phase, except for the duration (no change in orientation). In the Uncon-DEV condition, the orientation of the grating, which appeared “unconsciously,” changed by 90º. In the Con-DEV condition, the orientation of the grating, which was perceived “consciously,” was changed by 90º. Stimuli presented to both eyes in each trial were determined based on the perceptual report immediately prior to the target stimulus. The target stimulus was immediately followed by a cue image, which appeared for up to 3 seconds. In the cue image, the white fixation cross of the target stimulus was replaced with a green fixation cross for both the eyes. When green fixation appeared, the participants were asked to stop pressing the left arrow key or the right arrow key immediately. They were then required to promptly report their currently perceived grating image again by pressing either the left arrow key or the right arrow key, as in the task during the second phase. Upon pressing the key, the cue image disappeared. The inter-trial interval (ITI) was 2 seconds. During ITI, rings and green fixation points were exclusively presented. Each of the three conditions contained 120 trials. The order of these stimulus conditions was randomized across trials. There were eight sessions in the present study, each of which had 45 trials. Participants were given rest between sessions, as needed.

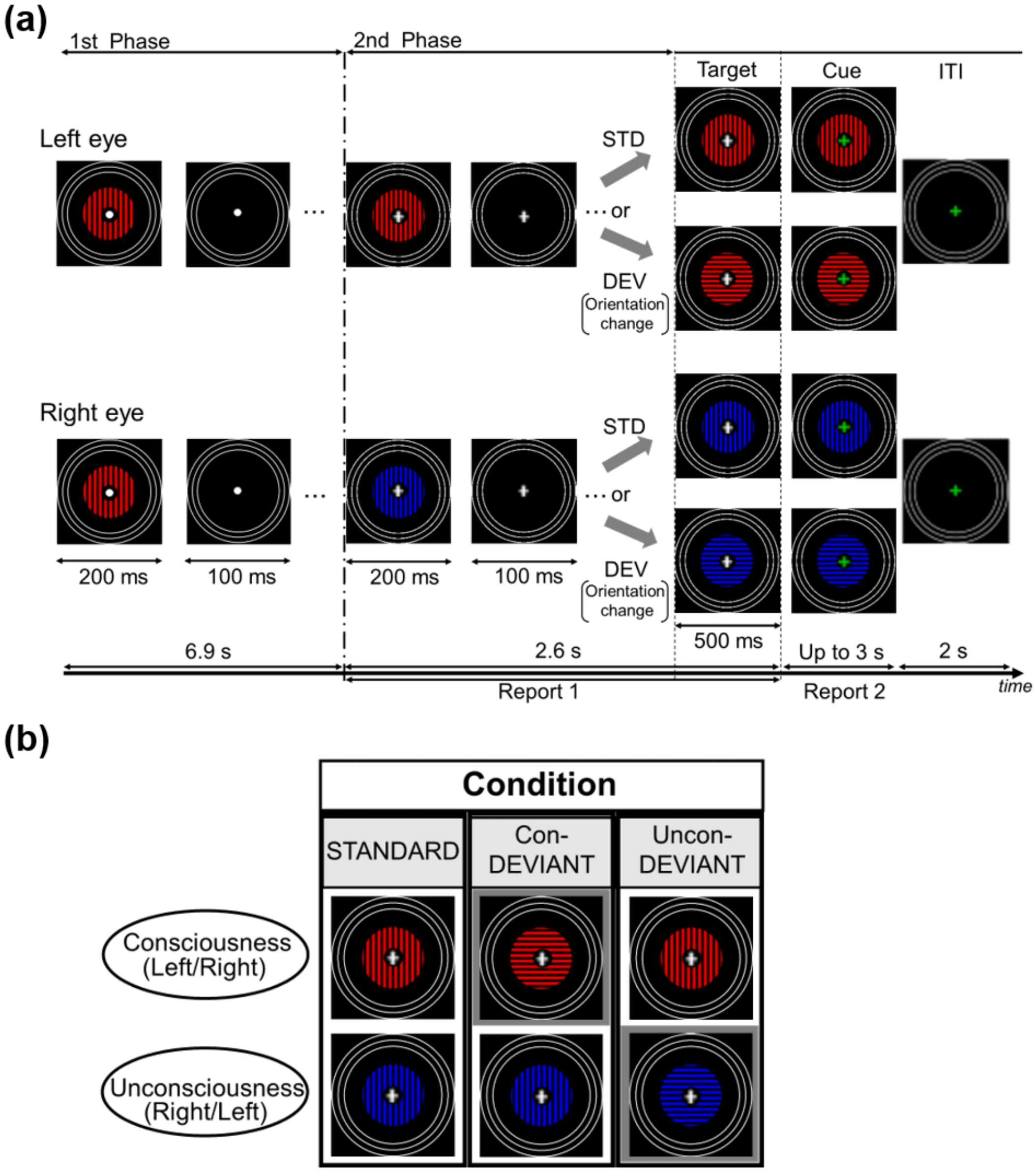

Figure 1. Time course of stimulus presentation and experimental conditions.

Stimulation paradigm for one trial was shown. Each trial consisted of two stimulation phases (a). Each pear of two grating stimuli arranged vertically indicates an example of target stimulus (b). Target stimulus had three variants by changing or not changing an orientation of the grating stimulus under the binocular rivalry. The same figure in Kurita et al. (2021) has been reproduced here.

3.1.3. Analysis of behavioral data

Under the current stimulation paradigm, the number of trials in which the perceived color changed after the target stimulus for each condition was obtained. Owing to the latency of the behavioral response, the timing of the participants' keypress would lag from the perceived rivalry changes by approximately 450–500 ms (Alais et al., 2010). In this analysis, we first counted the trials in which participants pressed a response key for at least 500 ms immediately before the onset of the target stimulus. We then subtracted the number of trials in which a participant did not stop pressing the key or did not press it again following the onset of the cue image. In this procedure, trials in which participants responded within 300 ms of the cue onset were also excluded to ensure that participants had correctly checked the cue. These procedures enabled us to obtain valid trials and count the number of times when the perceived color changed from before to after the onset of the target stimulus, and then calculated the proportion of perceptual alternation for every condition. The calculated proportions of perceptual alternation were submitted to a repeated-measures one-way analysis of variance (ANOVA) with a factor of the conditions (STD, Con-DEV, and Uncon-DEV conditions). Post-hoc tests were performed using Bonferroni correction. To confirm that the effects of the target stimulus on the proportion of perceptual alternation would not depend on a perceived grating prior to the presentation of the target stimulus, we further calculated the proportion of perceptual alternation for each direction of perceptual change (i.e., perceptual changes from the blue grating to the red grating, or vice versa) in every participant. The obtained proportions were then subjected to a repeated-measures two-way ANOVA with factors of the directions of perceptual change and conditions. In the statistical analyses, the significance level was set at $p < 0.05$.

3.1.4. EEG recording

EEG signal in each condition was recorded using a measurement instrument with 57 electrodes (EEG-1200, Nihon Kohden, Tokyo, Japan; EasyCap GmbH, Herrsching, Germany). The layout of the electrodes was based on a modified version of the international 10–20 system. The impedance of each electrode was maintained less than 10 kΩ. EEG signals were digitized at 1 kHz and recorded with a 0.5–300 Hz band-pass filter online. For data acquisition, EEG signals were referenced to the right earlobe and eye movements were monitored using horizontal and vertical bipolar electrooculograms (EOGs).

3.1.5. Analysis of EEG data

EEG signals were low-pass filtered offline at 30 Hz. EEG epochs from 100 ms before to 500 ms after the onset of the target stimulus in valid trials were collected (see Analysis of behavioral data for details). We then calculated the mean of the EEG epochs across trials to obtain VEPs which were time-locked to the target stimulus. In this calculation of VEPs, EEG epochs containing a deflection of greater than ±100 µV in at least one electrode, or of greater than 60 µV at EOGs, were excluded from averaging. With this procedure, at least 75 artifact-free EEG signals (mean ± SD, STD condition: 103.4 ± 12.5 trials, Uncon-DEV condition: 109.6 ± 8.41 trials, Con-DEV condition: 109.3 ± 10.5 trials) were averaged in each condition for each participant. The mean amplitude for a period of -100 to 0 ms relative to the stimulus onset was used as the baseline, and the obtained VEP was re-referenced to the average of all electrodes to be consistent with the previous studies (Urakawa et al., 2017a; Urakawa et al., 2018). Based on previous studies (e.g., Guthrie and Buchwald, 1991; Doniger et al., 2001; Urakawa et al., 2017a), the difference in the VEP amplitude at Oz electrode between the Con-DEV condition and the STD condition, as well as that between the Uncon-DEV condition and the STD condition, was respectively evaluated using a series of two-tailed *t*-tests through successive time points. When the *t*-tests exceeded the 0.05 criterion for at least 20 subsequent time points, the amplitude difference between the conditions was considered to be significant. To record vMMN evoked by the deviant presented under the unconscious condition (Uncon-vMMN) as well as that evoked by the deviant presented under the conscious condition (Con-vMMN), VEP to the target stimulus for the STD condition was subtracted from that to the target stimulus for the Uncon-DEV condition or from that to the target stimulus for the Con-DEV condition. In line with the previous studies (Urakawa et al., 2017a; Urakawa et al., 2018), vMMNs prominently appeared at Oz across participants for both the Uncon-vMMN and the Con-vMMN. The present study thus focused on vMMN at Oz. By using differential VEPs (Uncon-DEV/Con-DEV – STD) at Oz, we visually identified their negative peaks at the latencies 100 ms later than the target stimulus's onset. vMMN's latencies/amplitudes were then obtained; the first negative peak was identified as vMMN1's peak and the second negative peak was identified as vMMN2's peak. The difference in vMMN's peak latency/amplitude between the Uncon-vMMN and the Con-vMMN was evaluated using paired *t*-tests.

3.1.6. Correlation analysis

As in previous studies (Urakawa et al., 2017a; Urakawa et al., 2018), we further performed correlation analyses between the differential proportion of perceptual alternation (Uncon-DEV – STD or Con-DEV – STD) and peak latency/amplitude of vMMN across participants. The differential proportion was calculated by subtracting the proportions of perceptual alternation between the conditions, Uncon-DEV and STD or Con-DEV and STD. In the correlation analysis, absolute values of vMMN's amplitude were evaluated. The Spearman's rank order correlation coefficient was calculated. In the analyses, vMMN data that were not clearly identified upon visual inspection were excluded, and the significance level was set at $p < 0.05$.

3.2. Results

3.2.1. Behavioral data

Figure 2 shows the proportion of perceptual alternation from before to after the target stimulus. The mean proportions of perceptual alternation were 0.353 ± 0.035 (SE) for the STD condition, 0.039 ± 0.010 (SE) for the con-DEV condition, and 0.943 ± 0.016 (SE) for the Uncon-DEV condition. For each condition, none of the proportion values exceeded the range of the mean ± 3 SD. Repeated-measures one-way ANOVA revealed that the proportion was significantly affected by the conditions (F (2, 36) = 424.023, $p <$ 0.01, partial $\eta^2 = 0.959$). An analysis of multiple comparisons further revealed that the proportion in the Uncon-DEV condition was significantly higher than that in the STD condition (t (18) = 15.39, $p < 0.01$, Cohen's $d = 4.95$, post-hoc test with Bonferroni correction) and that the proportion in the Con-DEV condition was significantly lower than that in the STD condition (t (18) = 10.08, $p < 0.01$, Cohen's $d = 2.81$, post-hoc test with Bonferroni correction). There was also a significant difference in the proportion between the Uncon-DEV and Con-DEV conditions (t (18) = 38.87, $p < 0.01$, Cohen's $d =$ 15.43, post-hoc test with Bonferroni correction). These results indicate that the deviant on an unconsciously presented image is likely to render the unconscious image consciously perceived (i.e., the facilitation of the perceptual alternation) (Walker & Powell, 1979). In contrast, the deviant on a consciously presented image is likely to keep it perceived from before to after the presentation of the deviant (i.e., the suppression of perceptual alternation). In further analysis, we evaluated whether the proportion of perceptual change would be affected by perceived grating prior to the presentation of the target stimulus. For the STD condition, the mean proportion of perceptual change from blue to red gratings across participants was 0.210 ± 0.027 (SE), whereas that from the red grating to the blue grating was 0.143 ± 0.021 (SE). For the Con-DEV condition, the mean proportion of perceptual change from blue to red gratings was 0.014 ± 0.004 (SE), whereas that from red to blue gratings was 0.024 ± 0.007 (SE). For the Uncon-DEV condition, the mean proportion of perceptual change from blue to red gratings was 0.446 ± 0.029 (SE), whereas that from red to blue gratings was 0.498 ± 0.031 (SE). A repeated-measures two-way ANOVA revealed that the proportion was not significantly affected by the direction of perceptual change (F (1, 18) = .005, $p = 0.946$, partial $\eta^2 < 0.01$). There was no significant interaction between the conditions and the direction of perceptual change (F (2, 36) = 2.336, $p = 0.111$, partial $\eta^2 = 0.115$). These findings indicate that the proportion of perceptual alternation was unaffected by changes in consciously perceived color from before to after the onset of the target stimulus.

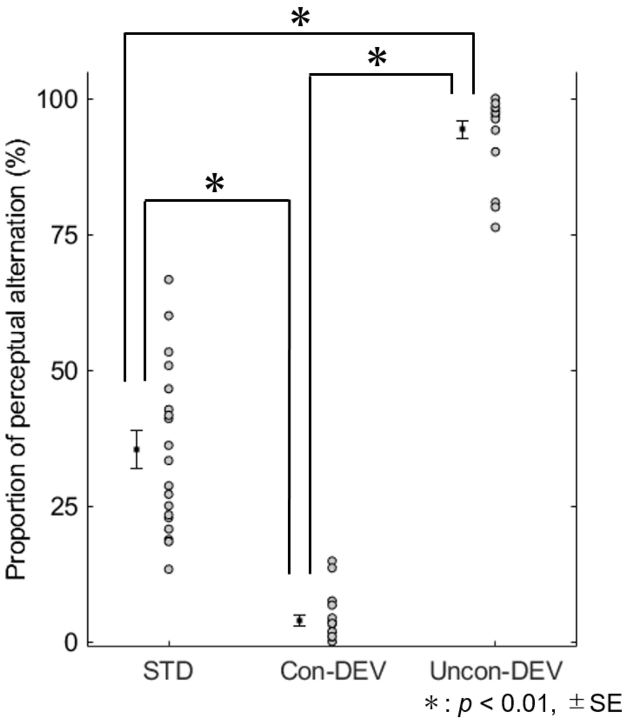

Figure 2. Proportion of perceptual alternation for each condition.

The proportion of perceptual alternation for all participants are shown for each condition. The mean proportion is indicated by black-filled square with ± SE. The same figure in Kurita et al. (2021) has been reproduced here.

3.2.2. EEG data

Figure 3 shows the grand-averaged VEP waveform at Oz and isocontour maps at latencies of 100 ms and 280 ms for each condition. The VEP amplitude appeared to be more negatively shifted for the Uncon-DEV condition or the Con-DEV condition than for the STD condition at Oz. Two-tailed *t*-tests through successive time points (see methods for details) revealed that the negative shift of VEP for the Uncon-DEV condition over the STD condition was significant at a latency of 115–334 ms. The enhancement of VEP for the Con-DEV over the STD condition was also significant at a latency of 114–362 ms.

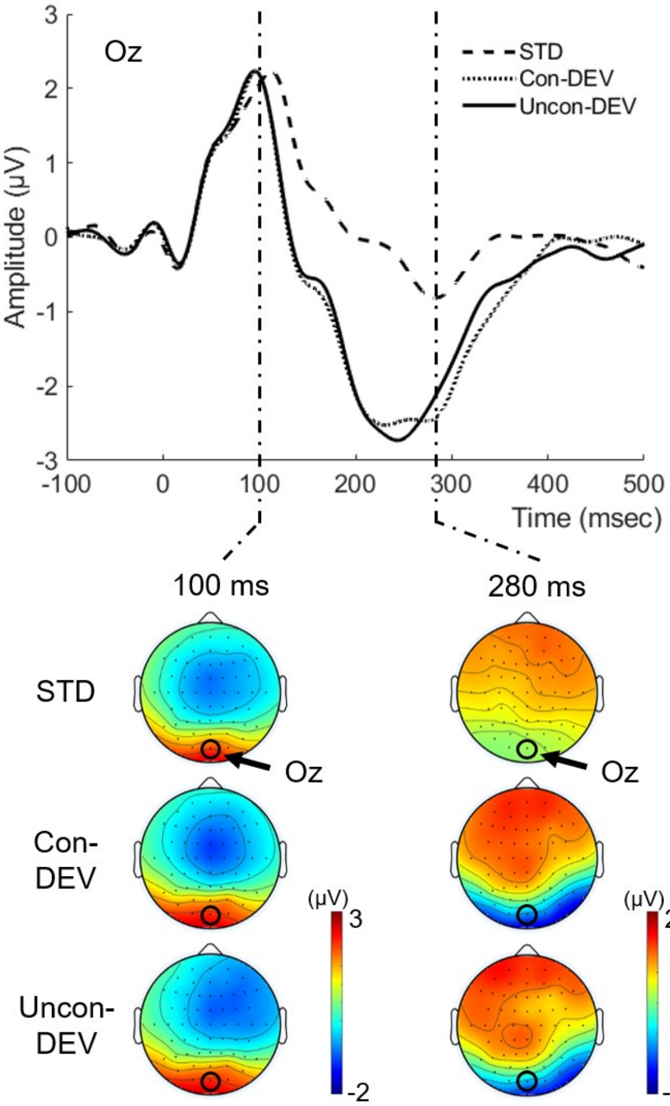

Figure 3. Grand-averaged VEPs to the target image for each condition.

VEPs at Oz and their isocontour maps at latencies of 100 and 280 ms were illustrated for each condition. VEPs in both the Con-DEV condition and the Uncon-DEV condition were more negatively enhanced than VEP in the STD condition at a latency range of approximately 100–400 ms. The same figure in Kurita et al. (2021) has been reproduced here.

Figure 4 shows the grand-averaged vMMNs (Con-vMMN and Uncon-vMMN) at Oz with their isocontour maps at latencies of 130 ms and 230 ms. In line with the previous studies (Urakawa et al., 2017a; Urakawa et al., 2018), the negative shift appeared at Oz particularly at a latency range of approximately 100–400 ms. As in previous studies (e.g., Maekawa et al., 2005), two successive peaks for posterior negativities (hereafter, we refer to the first negativity as vMMN1 and the second negativity as vMMN2) were observed at a latency of approximately 100–250 ms for both the Uncon-vMMN and the Con-vMMN. These findings support the fact that our current stimulation paradigm was effective in evoking vMMN.

For each vMMN1 and vMMN2, we evaluated the difference in the vMMN peak latency/amplitude between the Uncon-vMMN and the Con-vMMN. The vMMN2 data for three participants were excluded from analysis due to lack of prominent vMMN2 emergence. For vMMN1, the mean of peak latency was 145 ± 7.3 (SE) ms in the Uncon-vMMN and 147 ± 7.5 (SE) ms in the Con-vMMN. The mean of peak amplitude was -2.636 ± 0.356 (SE) μV in the Uncon-vMMN and -2.621 ± 0.315 (SE) μV in the Con-vMMN. Paired *t*-tests indicated that there was no significant difference in both peak latency and peak amplitude between the Uncon-vMMN and the Con-vMMN (for peak latency, *t* (18) = 0.832, *p* = 0.416, Cohen's *d* = 0.05; for peak amplitude, *t* (18) = 0.089, *p* = 0.930, Cohen's *d* = 0.01).

As for vMMN2, the mean of peak latency was 245 ± 6.6 (SE) ms in the Uncon-vMMN and 237 ± 5.1 ms (SE) in the Con-vMMN. Paired *t*-tests indicated that the Uncon-vMMN was significantly elongated in latency over the Con-vMMN (*t* (15) = 2.228, *p* = 0.042, Cohen's *d* = 0.35). The mean of peak amplitude was -2.777 ± 0.412 (SE) µV in the Uncon-vMMN and -2.664 ± 0.340 (SE) µV in the Con-vMMN. There was no significant difference in amplitude between the Uncon-vMMN and the Con-vMMN (t (15) = 0.523, p = 0.609, Cohen's *d* = 0.07).

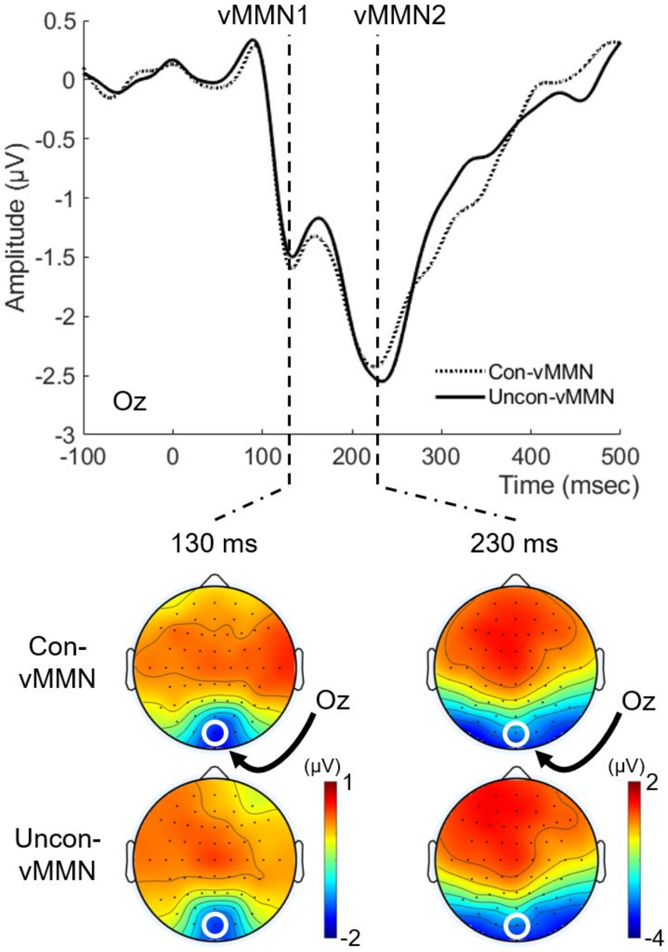

Figure 4. Grand-averaged vMMNs to the target image.

vMMN at Oz and topographical maps at latencies of 130 and 230 ms were shown for each condition. Two successive vMMNs (vMMN1 and vMMN2) emerged. vMMNs evoked in both the Uncon-DEV condition and the Con-DEV condition prominently appeared at Oz. The same figure in Kurita et al. (2021) has been reproduced here.

3.2.3. Correlation between behavioral data and vMMNs

With a focus on inter-individual variability in behavioral and neural data, we evaluated whether the Uncon-vMMN and the Con-vMMN would be relevant to the facilitation and suppression of the perceptual alternation, respectively. Figure 5a shows the results of correlation analyses for vMMN1. In the Con-vMMN, there was no significant relationship between the differential proportion of perceptual alternation and latency (ρ (19) = 0.131, p = 0.594) or amplitude (ρ (19) = 0.302, p = 0.209) across participants. As for the Uncon-vMMN, there was not a significant correlation between the differential proportion of perceptual alternation and latency (ρ (19) = 0.151, p = 0.537), there was a significant positive correlation between differential proportion and amplitude (ρ (19) = 0.517, p = 0.023), with an enhancement of the Uncon-vMMN significantly correlated with facilitation of the perceptual alternation across participants. Figure 5b shows the results of correlation analyses for vMMN2. In the Con-vMMN, there was no significant relationship between differential proportion and latency (ρ (16) = -0.032, p = 0.905) or amplitude (ρ (16) = 0.338, p = 0.200). As for the Uncon-vMMN, there was not significant correlation between differential proportion and latency (ρ (16) = 0.049, p = 0.858) or amplitude (ρ (16) = 0.386, p = 0.140). Considering these results, the peak amplitude of vMMN1 for the Uncon-DEV condition exclusively reflects perceptual alternation in a manner that the enhancement of the vMMN (the Uncon-vMMN) is relevant to rendering an unconsciously presented image perceived consciously. The correlation between Uncon-vMMN and perceptual alternation in the present study was consistent with those in the previous studies on perceptual alternation in Necker cube (Urakawa et al., 2017a; Urakawa et al., 2018). The number of participants for evaluating the individual differences in the present study was also comparable to the previous studies (10 – 20 participants).

VMMN was evoked by conscious and unconscious deviant stimuli. Our behavioral results showed that the conscious deviant stimulus suppressed perceptual alternation, while the unconscious deviant stimulus facilitated perceptual alternation. These EEG and behavioral results suggest that vMMN may be involved in making the deviant stimulus more perceptible, independent of whether the deviant was presented consciously or unconsciously. On the other hand, there was a significant correlation between the behavioral index and vMMN in the unconscious condition, although there was no significant difference in the conscious condition. These results indicate that the neural processing underlying vMMN is closely involved in the visual perceptual processing of the unconscious stimulus rather than the conscious stimulus. Thus, vMMN is related to APVA, which is an unconscious neural process.

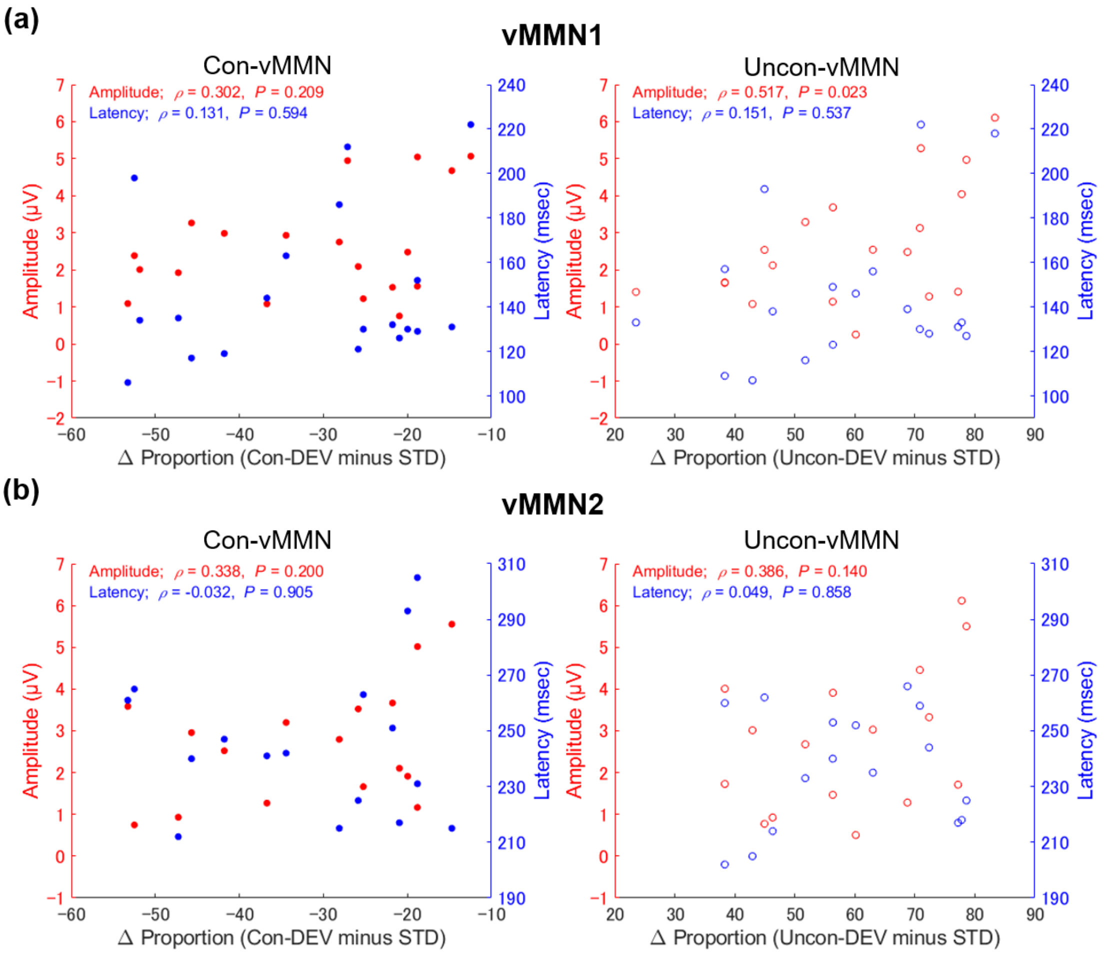

Figure 5. Relationship between proportion of perceptual alternation and vMMNs across participants.

The correlations between the differential proportion of perceptual alternation (Uncon-DEV condition – STD condition; Con-DEV condition – STD condition) and vMMN (Uncon-vMMN; Con-vMMN) are shown for vMMN1 (a) and vMMN2 (b). There was a significant correlation between differential proportion and an enhancement of the Uncon-vMMN. The same figure in Kurita et al. (2021) has been reproduced here.

3.3. Discussion

The Experiment 1 confirmed the hypothesis that vMMN reflecting the automatic visual change detection is relevant to APVA. The deviant stimulus of orientation change enabled us to discover the relationship between the perceptual alternation and vMMN. Consequently, we found a significant correlation between the enhancement of Uncon-vMMN's amplitude and the facilitation of perceptual alternation when the unconscious deviant was presented. On the other hand, no significant correlation was observed when the conscious deviant was presented. These results indicated that the unconscious visual processing underlying vMMN is involved in APVA.

Our current finding showed that the unconscious deviant, which was an external perturbation, made the unconscious stimulus more likely to be consciously perceived. This might originate from exogenous attention induced by the unconscious deviant. This reasoning is consistent with previous studies, which showed that exogenous attention to a certain location of the visual field facilitates visual processing to the invisible target image presented at the location; thus, the exogenous attention plays an important role in shaping conscious perception (Chica et al., 2010; Chica et al., 2011). Taken together, these results support our hypothesis that vMMN evoked by the unconscious deviant and its associated attentional mechanism make it easier for the unconscious stimulus to be consciously perceived.

Concerning vMMN2, the peak latency of Uncon-vMMN2 was significantly longer than that of Con-vMMN2 (see EEG data in Results in Experiment 1). In vMMN latency, we should take VAN into account. This is because VAN is observed at a peak latency of approximately 200 ms after the stimulus onset when the visual stimulus is consciously perceived (Koivisto & Revonsuo, 2003; Koivisto & Grassini, 2016). In the present study's results, the proportion of perceptual alternation in the Uncon-DEV condition was very high, at about 95%, and the unconscious visual stimulus was almost consciously perceived. Therefore, it is highly likely that VAN, which is related to the conscious perception of the visual stimulus, emerged in the Uncon-vMMN2 and affected peak latency.

In summary, the results showed a correlation between the enhancement of vMMN amplitude and the facilitation of perceptual alternation in binocular rivalry when an unconscious deviant was presented. This implies that vMMN, which reflects an automatic visual change detection, is relevant to APVA. In early visual processing, the attentional mechanism associated with vMMN is suggested to play an important role in APVA. The discovered relevance of vMMN on APVA is a significant first step in elucidating early unconscious processing before established conscious perception.

4. Experiment 2: The role of mismatch process in AVPA

To investigate the effects of oscillatory brain activities based on visual mismatch process on APVA, we further analyzed the theta band ERSP and ITPC for the EEG data in Experiment 1. This is expected to clarify whether neural processing related to vMORs, which is little known so far, is involved in APVA. This chapter describes the analysis methods, results, and discussions of Experiment 2. The experimental procedures and recorded EEG data are the same as Experiment 1. Contents of this chapter is also described in the paper (Kurita et al., 2023).

4.1. Methods

The subjects, stimulus and procedure, analysis of behavioral data, and EEG recording methods were same as those in Experiment 1. Analytical methods such as ERSP and ITPC were additionally executed to reach the goal.

4.1.1. Analysis of EEG data

EEG epochs from 400 ms before to 600 ms after the onset of the target stimulus in valid trials were collected. EEG epochs containing a deflection greater than ±100 μV in at least one electrode or greater than 100 μV in EOGs were excluded from this analysis. With this procedure, at least 77 artifact-free EEG epochs (mean ± SD, STD condition: 105.2 ± 11.8 trials, Con-DEV condition: 104.6 ± 13.0 trials, Uncon-DEV condition: 104.9 ± 8.7 trials) were obtained. These epochs were sorted according to the target stimulus conditions and then transformed into time-frequency representations via a complex Morlet wavelet transformation using the wavelet toolbox in the MATLAB psycho-toolbox 3 (Brainard, 1997; Pelli, 1997). Then we calculated ERSP and ITPC for each stimulus condition using the MATLAB wavelet toolbox. ITPCs were calculated by summation of phase angles of all epochs for each time point and in each electrode (Tallon-Baudry et al., 1996; Van Diepen & Mazaheri, 2018). ERSP was calculated by summation of squared amplitudes of all epochs for each time point and in each electrode (Makeig, 1993; Grandchamp & Delorme, 2011). In this time-frequency analysis, cycles of the mother wavelet were set to a linear increase of 2–7 cycles with respect to the frequency range (1–50 Hz). The ERSP and ITPC of each participant were calculated relative to the baseline (-400 to -100 ms) for each electrode. To record vMORs evoked by the unconscious deviant (Uncon-vMORs) as well as those evoked by the conscious deviant (Con-vMORs), ERSP and ITPC in the STD condition were subtracted from those in the Uncon-DEV and Con-DEV conditions, respectively. For both Con-vMORs and Uncon-vMORs, the ERSP and ITPC in the left area (PO3, PO7) and right area (PO4, PO8) were calculated for each participant in the time-frequency window of 100–500 ms and 4–8 Hz, respectively. This time-frequency window was determined in previous studies on vMORs (Stothart et al., 2013; Yan et al., 2017). The calculated ERSP and ITPC were subjected to a repeated-measures two-way ANOVA with factors of the conditions (Con-vMOR and Uncon-vMOR) and laterality (left and right areas). In the statistical analyses, the significance level was set at $p < 0.05$.

4.1.2. Correlation analysis

As in the Experiment 1, we further performed correlation analyses between the differential proportion of perceptual alternation and ERSP/ITPC of vMORs (Con-vMORs or Uncon-vMORs) across participants. The differential proportion was calculated by subtracting the proportions of perceptual alternation between the conditions; Con-DEV and STD, or Uncon-DEV and STD. The data under the conscious and unconscious conditions are considered to be statistically independent because the stimuli are completely different. The Spearman's rank-order correlation coefficients were calculated. In the analyses, the significance level was set at $p < 0.05$.

4.2. Results

Results of behavioral data in the Experiment 2 are common to the results of the Experiment 1 (see Behavioral Data in *Experiment 1* and Figure 2).

4.2.1. EEG data

Figure 6 shows the averaged ERSP and ITPC in the posterior area (PO3, PO7, PO4, PO8) and the averaged isocontour map in the time-frequency window for each condition. In the time-frequency window, ERSP and ITPC in the theta band appear to be enhanced by approximately 100–500 ms for the Con-DEV condition or the Uncon-DEV condition than for the STD condition in the posterior area. These results are consistent with those of previous studies on vMORs (Stothart et al., 2013; Yan et al., 2017).

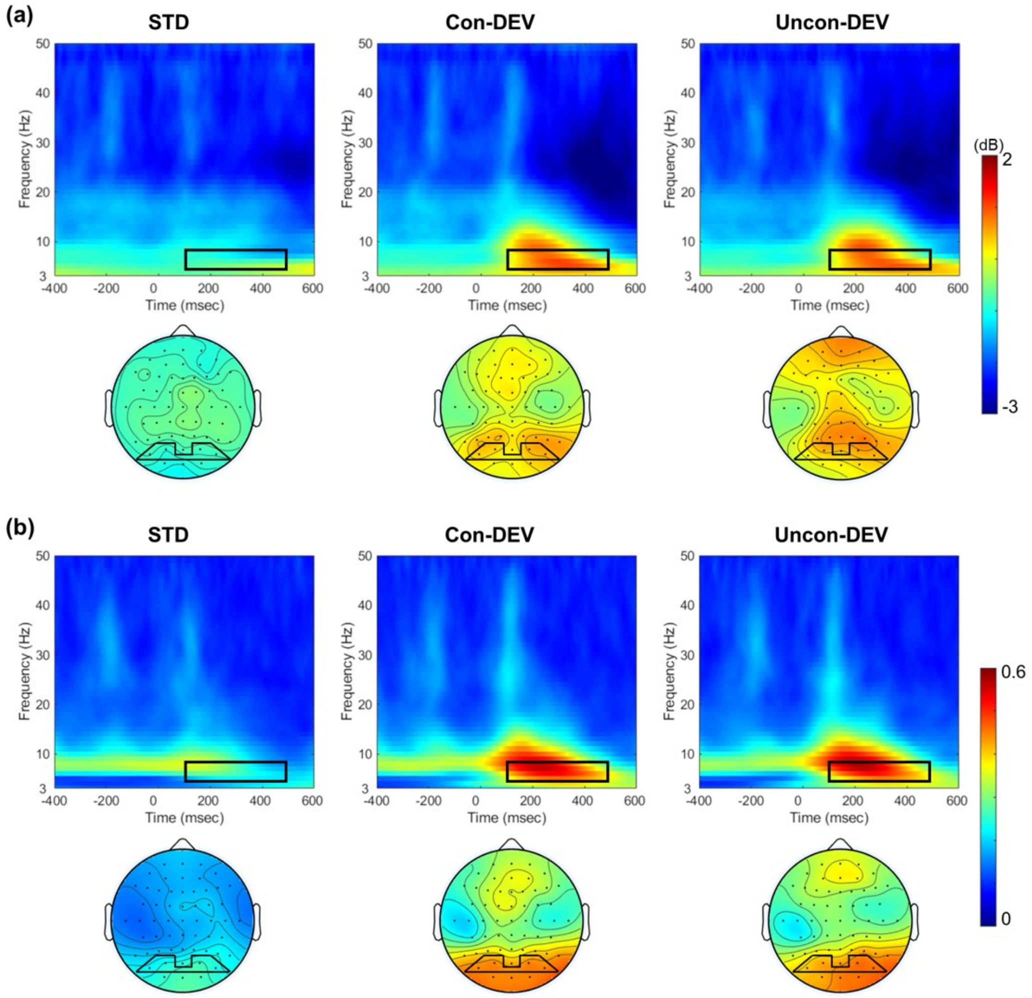

Figure 6. ERSP and ITPC to the target image for each target condition.

ERSPs (a) and ITPCs (b) at the posterior area (PO3, PO7, PO4, and PO8) and their isocontour maps averaged from 4 to 8 Hz at 100 to 500 ms are illustrated for each condition. ERSPs and ITPCs in both the Con-DEV and Uncon-DEV conditions were more enhanced than those in the STD condition in the time-frequency windows of 100–500 ms and 4–8 Hz. The same figure in Kurita et al. (2023) has been reproduced here.

Figure 7 shows ERSPs of Con-vMORs and Uncon-vMORs in the right and left areas, respectively, and the averaged isocontour map in the time-frequency window. An increase in ERSP was observed at 6–8 Hz between approximately 200–400 ms, for both the Con-vMOR and the Uncon-vMOR. A repeated-measures two-way ANOVA revealed that the enhancement of ERSP was not significantly affected by the condition and laterality (Condition: F (1, 18) = .003, p = 0.956, partial $\eta^2 < 0.01$; Laterality: F (1, 18) = .245, p = 0.626, partial $\eta^2 = 0.013$), or interaction (F (1, 18) = .429, p = 0.521, partial $\eta^2 = 0.023$). These results indicated that the increase of theta band ERSP by the deviant stimulus is independent of whether the deviant stimulus is presented consciously or unconsciously, and that there is no significant difference in the increase of ERSP between the left and right areas.

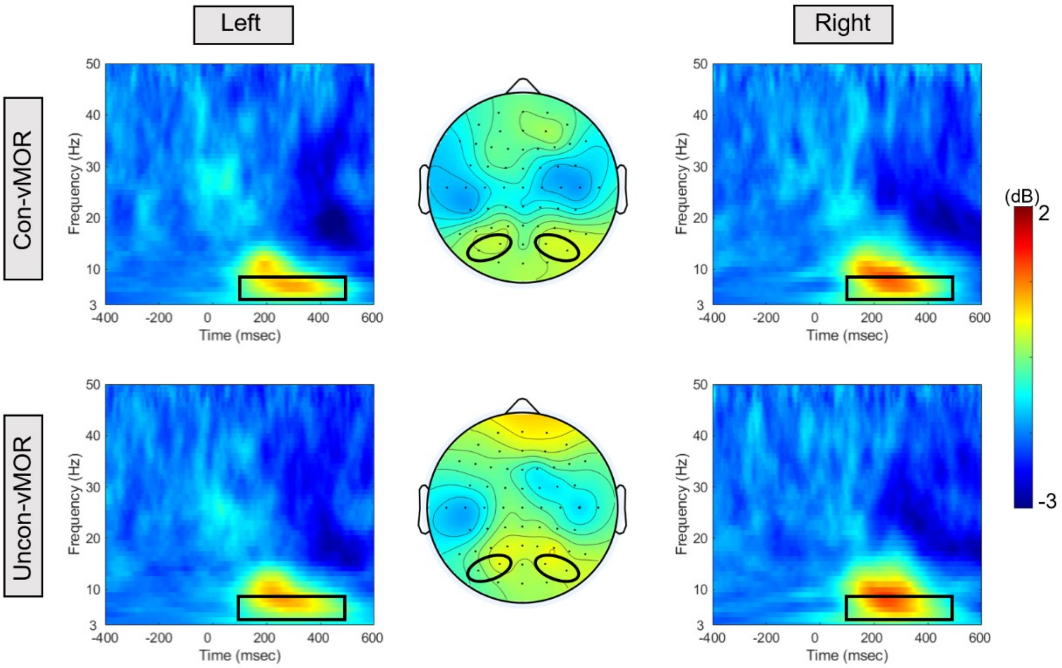

Figure 7. ERSPs and their isocontour map for each condition.

The panels show the ERSPs in the Con-vMOR condition in the left area (PO3, PO7) (upper left panel), the Con-vMOR condition in the right area (PO4, PO8) (upper right panel), the Uncon-vMOR condition in the left area (lower left panel), the Uncon-vMOR condition in the right area (lower right panel), and their isocontour maps (the upper map is in the Con-vMOR condition, and the lower map is in the Uncon-vMOR condition). The black box in the ERSPs indicates a time-frequency window of 100–500 ms and 4–8 Hz. The same figure in Kurita et al. (2023) has been reproduced here.

Figure 8 shows ITPCs of Con-vMORs and Uncon-vMORs in the right and left areas, respectively, and the averaged isocontour map in the time-frequency window. An increase in ITPC was observed at 6–8 Hz between approximately 200–400 ms for both the Con-vMOR and the Uncon-vMOR. A repeated-measures two-way ANOVA revealed that the enhancement of ITPC was not significantly affected by the condition or laterality (Condition: F (1, 18) = .377, p = 0.547, partial η^2 = 0.021; Laterality: F (1, 18) < .001, p = 0.985, partial η^2 < 0.01), and that the enhancement of ITPC was significantly affected by the interaction between the condition and the laterality (F (1, 18) = 14.695, p < 0.01, partial η^2 = 0.449). An analysis of multiple comparisons further revealed that the ITPC in the left area under the Uncon-vMOR condition was marginally and significantly lower than that under the Con-vMOR condition (Condition in Left: F (1, 18) = 3.211, p = 0.090, partial η^2 = 0.151), and the other simple main effects were not significant (Condition in Right: F (1, 18) = .754, p = 0.397, partial η^2 = 0.040; Laterality in Con-vMOR: F (1, 18) = .488, p = 0.494, partial η^2 = 0.026; Laterality in Uncon-vMOR: F (1, 18) = .619, p = 0.442, partial η^2 = 0.033). These results indicate that the increase of theta band ITPC in the left area by the deviant stimulus tends to differ depending on whether the deviant stimulus is presented consciously or unconsciously.

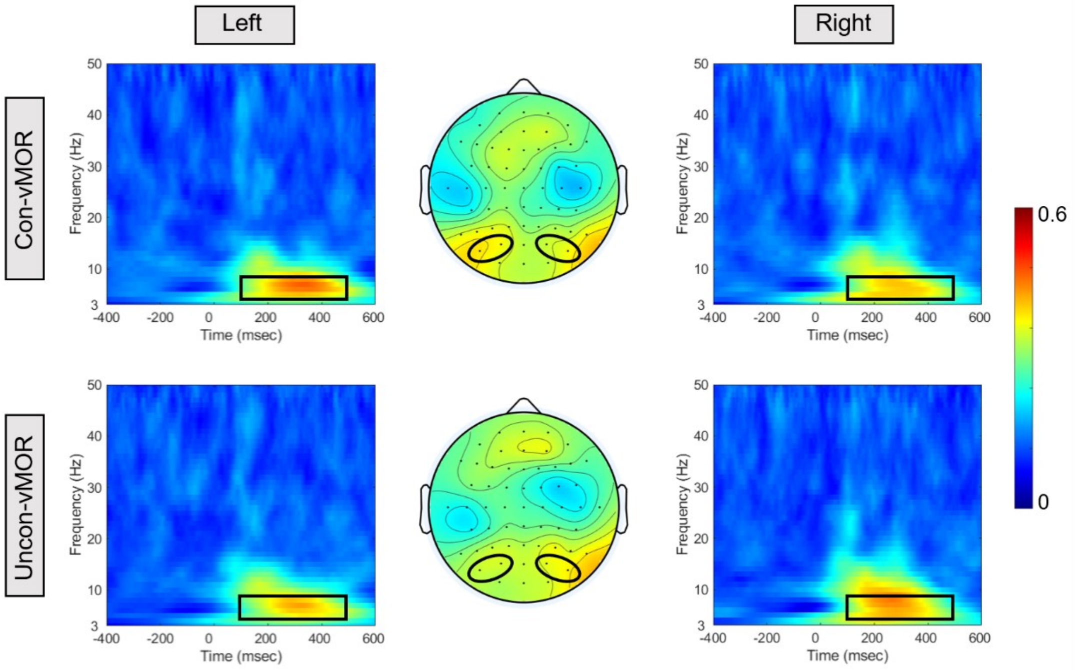

Figure 8. ITPCs and their isocontour map for each condition.

The panels show the ITPCs in the Con-vMOR condition in the left area (PO3, PO7) (upper left panel), the Con-vMOR condition in the right area (PO4, PO8) (upper right panel), the Uncon-vMOR condition in the left area (lower left panel), the Uncon-vMOR condition in the right area (lower right panel), and their isocontour maps (the upper map is in the Con-vMOR condition, and the lower map is in the Uncon-vMOR condition). The black box in the ITPCs indicates a time-frequency window of 100–500 ms and 4–8 Hz. The same figure in Kurita et al. (2023) has been reproduced here.

4.2.2. Correlation between behavioral data and vMORs

Focusing on the inter-individual variability in behavioral data and ERSP/ITPC in the left and right areas under the Con-vMOR and Uncon-vMOR conditions, respectively, we evaluated whether the ERSP/ITPC of vMORs in the theta band would be relevant to the facilitation or suppression of perceptual alternation. Figure 9 shows the results of the correlation analysis for ERSP and ITPC. For ERSP, there was no significant correlation between the differential proportion of perceptual alternation and ERSP in either condition (Con-vMOR on the left: ρ (19) = -0.021, p = 0.934; Con-vMOR on the right: ρ (19) = 0.016, p = 0.951; Uncon-vMOR on the left: ρ (19) = 0.139, p = 0.571; Uncon-vMOR on the right: ρ (19) = 0.201, p = 0.409). We analyzed the four correlations between ITPC and the differential proportion of perceptual alternation (Con-vMOR on the left: ρ (19) = 0.209, p = 0.389; Con-vMOR on the right: ρ (19) = 0.051, p = 0.837; Uncon-vMOR on the left: ρ (19) = 0.507, p = 0.027; Uncon-vMOR on the right: ρ (19) = 0.271, p = 0.261). In the correlation analyses for ITPC, we corrected for multiple tests for laterality (left and right areas) with a Bonferroni correction. As a result, there was a marginally significant positive correlation between the differential proportion of perceptual alternation and ITPC in the left area in the Uncon-vMOR condition. These results show that an enhancement of theta band ITPC in the left area by the unconscious deviant stimulus is correlated with facilitation of perceptual alternation across participants. Considering these results, an increase in the theta band ITPC in the left posterior area is more closely related to rendering an unconsciously presented image perceived consciously than that of ERSP.

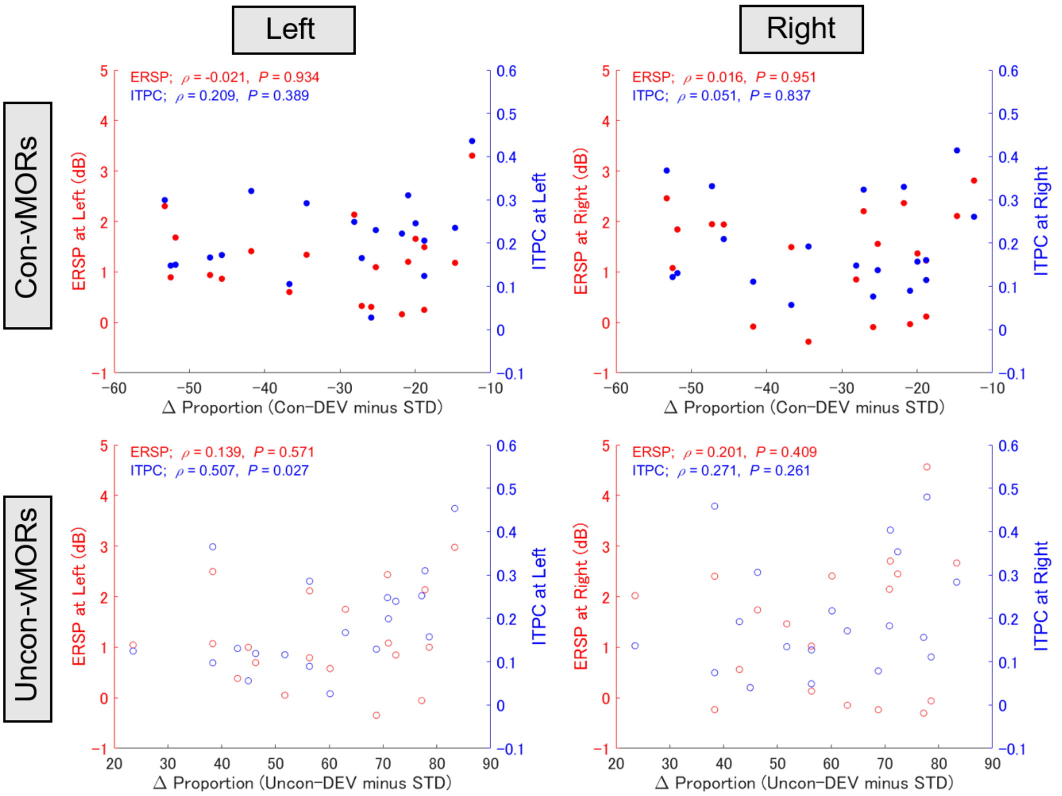

Figure 9. Relationship between proportion of perceptual alternation and vMORs across participants.

The correlations between the differential proportion of perceptual alternation (Uncon-DEV condition – STD condition; Con-DEV condition – STD condition) and ERSP/ITPC of vMORs in the theta band are shown for each condition (Con-vMOR in left: upper left panel; Con-vMOR in right: upper right panel; Uncon-vMOR in left: lower left panel; Uncon-vMOR in right: lower right panel). This figure is a modified version of the figure in Kurita et al. (2023).

4.3. Discussion

The Experiment 2 attempted to clarify whether vMORs in the theta band are related to APVA. We presented the deviant stimulus under binocular suppression or dominance and then investigated the relationship between perceptual alternation and ERSP or ITPC in the theta band. Consequently, we found a marginally significant positive correlation between the facilitation of perceptual alternation and an increase in ITPC at left side when the deviant stimulus was presented unconsciously. However, no significant correlation was observed in ERSP. These results indicate that phase alignment in the theta band underlying the visual mismatch process is involved in APVA.

A relationship between perceptual alternation and theta band ITPC in the left posterior area was observed under the Uncon-vMOR condition. According to the ANOVA for ITPC (see EEG data section), the posterior ITPC in the left hemisphere under the Uncon-vMOR condition tended to be lower than that under the Con-vMOR condition. Despite the smaller quantity of ITPC, the results showed that the left posterior theta ITPC evoked by unconscious deviant stimuli is only relevant to the facilitation of perceptual alternation. A previous study reported that theta oscillations in the left paracentral lobule encoded the resolution of conflicts induced by both stimulus-related conscious and unconscious information process (Giller et al., 2020). Similarly, in binocular rivalry, theta oscillatory activity in the left hemisphere is considered to be involved in neural processing, which determines conscious perception by solving the conflict between conscious and unconscious information. Therefore, these results indicate that the theta band posterior ITPC in the left hemisphere is relevant to the unconscious process of determining perceptual alternation in binocular rivalry.

We found that the increase in theta ITPC evoked by the unconscious deviant stimulus at the occipital electrodes tended to make it easier for the stimulus to be consciously perceived. Several studies have suggested that neural theta phase coherence in the visual mismatch process reflects information flow through functional connectivity, not only within the occipital sites, where vMMN is evoked by preattentive visual change detection, but also between the frontal and other areas, where the attentional mechanism associated with vMMN is involved (Stothart et al., 2013; MacLean and Ward, 2014; Hedge et al., 2015). From a theoretical viewpoint, top-down prediction as well as bottom-up stimulus information is indispensable for mismatch neural processing (Winkler and Czigler, 2012; Kimura, 2012). Thus, theta alignment associated with vMMN in the occipital areas may also reflect functional connectivity to the attentional mechanism in the prefrontal cortex. However, since our current finding comes from not synchronization between brain regions but ITPC at posterior area, it is not necessarily true that the functional connection between the occipital and frontal regions is involved in the promotion of consciousness perception. Taken together, these results indicate that the theta phase coherence evoked by the visual mismatch process plays an important role in the neural mechanism of APVA. This suggests that theta synchronization between frontal and posterior regions evoked by the unconscious deviant stimulus and the accompanying enhancement of the attentional mechanism make the unconscious stimulus easier to be consciously perceived.

5. Experiment 3: Effect of change-related response on APVA

To clarify whether change-related response affects APVA, we examined the correlation between change-related N1 and the perceptual alternation in binocular rivalry. Change-related N1 was observed by presenting sudden stimulus changes without temporal regularity in binocular rivalry. This correlation analysis is expected to clarify whether a neural activity associated with stimulus changes without temporal regularity affect APVA as well as vMMN. This chapter describes the experimental procedures, analysis methods, results, and discussions of Experiment 3.

5.1. Methods

5.1.1. Subjects

Nineteen healthy volunteers (14 males and 5 females, age 20–26 years, mean ± SD, 22.0 ± 1.49 years) participated in this experiment. Eighteen participants were right-handed and one participant was left-handed. All the participants had normal or corrected-to-normal visual acuity. Informed consent was obtained from all participants, and this experiment was approved by the ethics committee of Tokyo University of Science.

5.1.2. Stimulus and Procedure

Images were presented on a liquid crystal display (BenQ XL2540) using the MATLAB Psychophysics Toolbox (Brainard, 1997; Pelli, 1997). The participants were presented with two computer-generated images using a mirror stereoscope. The image included annulus-shaped gratings with a spatial frequency of 1.7 cycles/degree. The outer radius of the gratings was 3.2° and the inner radius was 0.38°. A white fixation point was presented at the center of the grating image. The blue or red grating was presented on a black background, with the same luminance in the Experiment 1. Each grating was surrounded by three white rings that served to lock the vergence. Each white ring had a line width of 0.13°. The outer radius of the largest ring was 5.76°, and the outer edges of each of the other two smaller rings were inwardly depicted by 0.64° from the outer edge of the neighboring larger ring. White rings in both eyes were continuously presented throughout the stimulation period.

Figure 10 shows the stimuli and the stimulation procedure for one trial and each trial had two consecutive phases same as Experiment 1. In the first phase, an identical grating image was simultaneously presented for 2.6 s to both the left and right eyes. The grating was either blue or red, and its orientation was either horizontal or vertical. Participants were asked to look at the fixation point passively. In the second phase, different color gratings (red or blue) were simultaneously presented for 1.4 s to each eye. The color was counterbalanced between the two eyes. During the second phase, a white fixation cross appeared at the center of the grating image instead of the white fixation point. When the white cross appeared, the participants were required to fixate on the cross and press a key on the keyboard in front of them to start reporting a perceived color of the grating image. Following the second phase, the target stimulus was immediately presented for 500 ms. The orientation of one of the target stimuli presented to both eyes abruptly changes (from horizontal to vertical or vice versa). The target stimulus yielded three conditions dependent on the subject's conscious/unconscious percept just before itself: the Control condition, the unconscious-change (Uncon-Change) condition, and the conscious-change (Con-Change) condition. In the Control condition, the target stimulus was the same as the grating images used in the second phase (no change in orientation). In the Uncon-Change condition, the orientation of the grating, which appeared "unconsciously," changed by 90º. In the Con-Change condition, the orientation of the grating, which was perceived "consciously," was changed by 90º. Stimuli presented to both eyes in each trial were determined based on the perceptual report immediately prior to the target stimulus. The target stimulus was immediately followed by a cue image, which appeared for up to 3 seconds. In the cue image, the white fixation cross of the target stimulus was replaced with a green fixation cross for both the eyes. When green fixation appeared, the participants were asked to stop pressing the left arrow key or the right arrow key immediately. They were then required to promptly report their currently perceived grating image again. Upon pressing the key, the cue image disappeared. The ITI was 2 seconds. During ITI, rings and green fixation points were exclusively presented. Each of the three conditions contained 160 trials. The order of these stimulus conditions was randomized across trials. There were eight sessions in the present study, each of which had 60 trials. Participants were given rest between sessions, as needed.

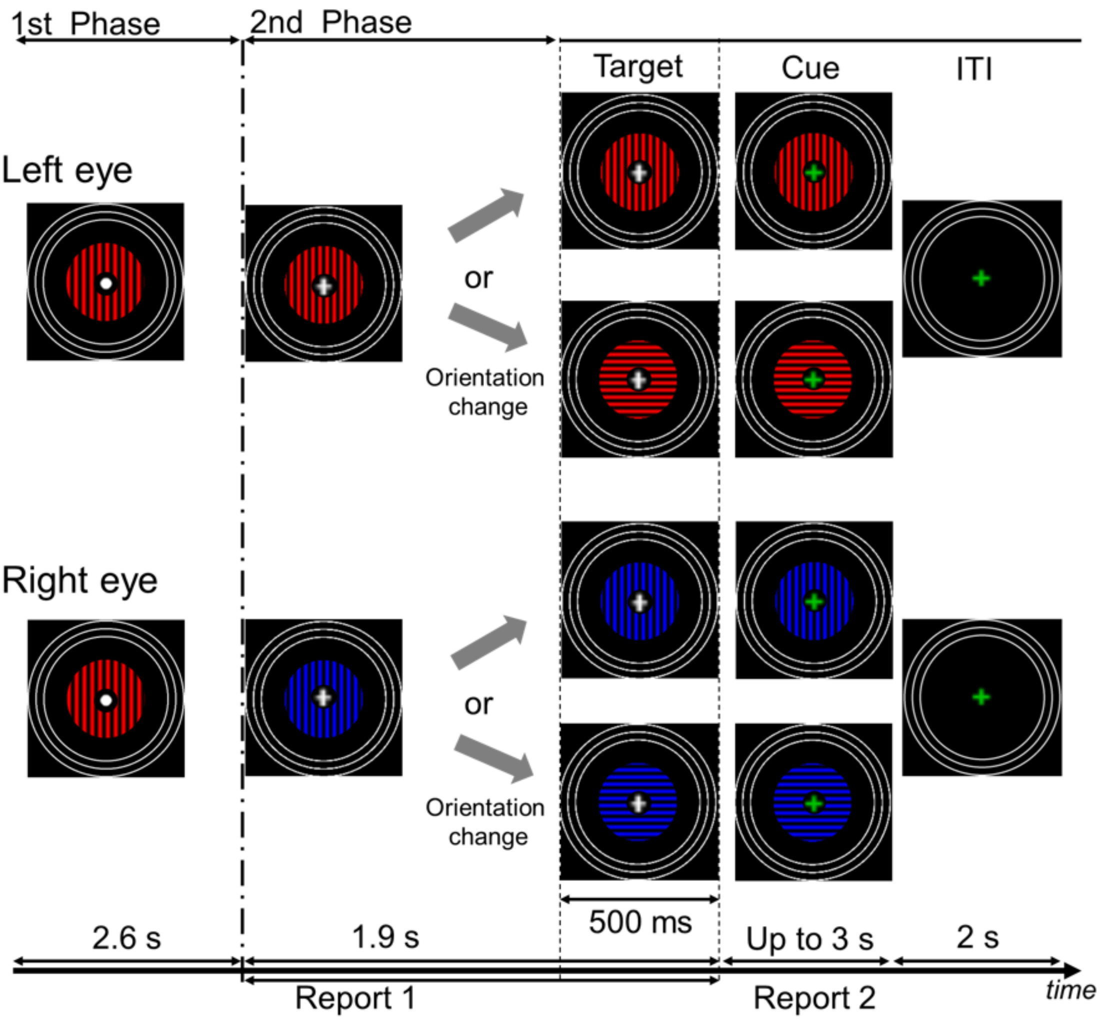

Figure 10. Time course of stimulus presentation in Experiment 3.

Stimulation paradigm for one trial was shown. Each trial consisted of two stimulation phases. Target stimulus yielded three conditions; Control, Con-Change, Uncon-Change. In the Uncon-Change condition, an orientation of the grating stimulus which was not perceived was exclusively changed by 90º. Meanwhile, in the Con-Change condition, an orientation of the grating stimulus which was perceived was exclusively changed by 90º. In the Control condition, there was no change of the grating stimulus for both eyes.

5.1.3. Analysis of behavioral data

We counted the trials in which participants pressed a response key for at least 500 ms immediately before the onset of the target stimulus. We then subtracted the number of trials in which a participant did not stop pressing the key or did not press it again following the onset of the cue image. In this procedure, trials in which participants responded within 300 ms of the cue onset were also excluded to ensure that participants had correctly checked the cue. These procedures enabled us to obtain valid trials and count the number of times when the perceived color changed from before to after the onset of the target stimulus, and then calculated the proportion of perceptual alternation for every condition. The proportions of perceptual alternation were submitted to a repeated-measures one-way ANOVA with a factor of the conditions (the Control, Con-Change, and Uncon-Change conditions). Post-hoc tests were performed using Bonferroni correction. In the statistical analyses, the significance level was set at $p < 0.05$.

5.1.4. EEG recording

EEG signals in each condition were recorded using a measurement instrument with 57 electrodes (EEG-1200, Nihon Kohden, Tokyo, Japan; EasyCap GmbH, Herrsching, Germany). The layout of the electrodes was based on a modified version of the international 10–20 system. The impedance of each electrode was maintained less than 10 kΩ. EEG signals were digitized at 1 kHz and recorded with a 0.5–300 Hz band-pass filter online. For data acquisition, EEG signals were referenced to the right earlobe and eye movements were monitored using horizontal and vertical bipolar EOGs. A nose tip signal was also recorded for re-reference in offline.

5.1.5. Analysis of EEG data

EEG signals were low-pass filtered offline at 30 Hz. EEG epochs from 100 ms before to 500 ms after the onset of the target stimulus in valid trials were collected. We then calculated the mean of the EEG epochs across trials to obtain VEPs which were time-locked to the target stimulus. In this calculation of VEPs, EEG epochs containing a deflection of greater than ±150 µV in at least one electrode, or of greater than 100 µV at EOGs, were excluded from averaging. With this procedure, at least 67 artifact-free EEG signals (mean ± SD, Control condition: 125.3 ± 21.9 trials, Uncon-DEV condition: 128.2 ± 24.6 trials, Con-DEV condition: 129.9 ± 23.6 trials) were averaged in each condition for each participant. The mean amplitude for a period of -100 to 0 ms relative to the stimulus onset was used as the baseline, and the obtained VEP was re-referenced to the nose tip signal. To extract Change-related N1 component under the unconscious and conscious condition, VEP at PO7 and PO8 for the Control condition was subtracted from that for the Uncon-Change condition (ΔUncon-Change) or from that for the Con-Change condition (ΔCon-Change). By using the differential VEPs, we visually identified the most negative peak for each participant at the closest latency of 200 ms after the stimulus onset as participant's change-related N1 latency/amplitude. The difference in the N1's peak latency/amplitude under the ΔUncon-Change and ΔCon-Change condition was evaluated using paired *t*-tests.

5.1.6. Correlation analysis

As in the previous study (Kurita et al., 2021), we performed correlation analyses between the differential proportion of perceptual alternation (Uncon-Change – Control or Con-Change – Control) and peak latency/amplitude of N1 across participants. The differential proportion was calculated by subtracting the proportions of perceptual alternation between the conditions, Uncon-Change and Control or Con-Change and Control. In the correlation analysis, absolute values of N1 amplitude were evaluated. The Spearman's rank order correlation coefficient was calculated. In the analyses, the significance level was set at $p < 0.05$.

5.2. Results

5.2.1. Behavioral data

Figure 11 shows the proportion of perceptual alternation for each condition. The mean proportions of perceptual alternation were 0.361 ± 0.042 (SE) for the Control condition, 0.076 ± 0.022 (SE) for the Con-Change condition, and 0.859 ± 0.047 (SE) for the Uncon-Change condition. For each condition, none of the proportion values exceeded the range of the mean ± 3 SD. Repeated-measures one-way ANOVA revealed that the proportion was significantly affected by the conditions (F (2, 36) = 109.025, $p < 0.01$, partial η^2 = 0.858). An analysis of multiple comparisons further revealed that the proportion in the Uncon-Change condition was significantly higher than that in the Control condition (t (18) = 9.47, $p < 0.01$, Cohen's d = 2.58, post-hoc test with Bonferroni correction) and that the proportion in the Con-Change condition was significantly lower than that in the Control condition (t (18) = 6.27, $p < 0.01$, Cohen's d = 1.96, post-hoc test with Bonferroni correction). There was also a significant difference in the proportion between the Uncon-Change and Con-Change conditions (t (18) = 12.68, $p < 0.01$, Cohen's d = 4.92, post-hoc test with Bonferroni correction). These results indicate that the sudden unconscious change of visual stimulus facilitated the perceptual alternation. In contrast, the sudden conscious change suppressed the perceptual alternation. These tendency of the results that the proportion of perceptual alternation decreases under the conscious stimulation condition and increases under the unconscious stimulation condition are consistent with the behavioral results in Experiment 1.

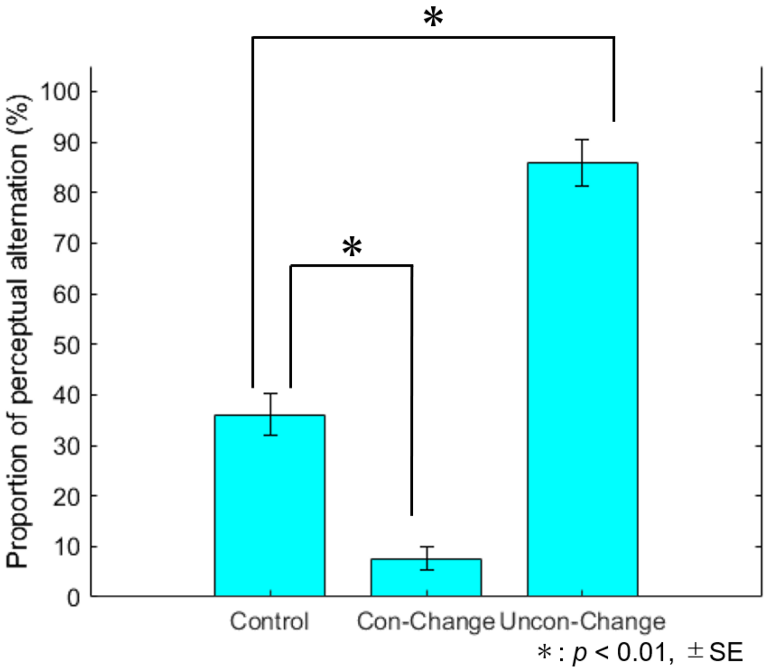

Figure 11. Mean proportion of perceptual alternation for each condition.

The mean proportion of perceptual alternation are shown for each condition. The proportion was significantly higher in the Uncon-Change condition than that in the Control condition. In contrast, the proportion was significantly lower in the Con-Change condition than that in the Control condition.

5.2.2. EEG data

Figure 12 shows the grand-averaged VEP waveform at PO7/8 and isocontour maps at latencies of 200 ms for (a) each condition and (b) subtracted condition. The change-related N1 was observed at PO7/8 at latencies of approximately 200 ms for the ΔUncon-Change and ΔCon-Change condition. These results show that our current stimulation paradigm was effective in evoking N1 by the sudden change of visual stimulus.

We evaluated the difference across participants in the N1 peak latency/amplitude between the ΔUncon-Change and ΔCon-Change condition by paired t-tests. The mean of N1 peak latency was 199 ± 4.4 (SE) ms in the ΔUncon-Change and 197 ± 4.2 (SE) ms in the ΔCon-Change. The mean of N1 peak amplitude was -8.43 ± 0.925 (SE) µV in the ΔUncon-Change and -8.20 ± 1.02 (SE) µV in the ΔCon-Change. Paired *t*-tests indicated that there was no significant difference in both peak latency and peak amplitude between the ΔUncon-Change and the ΔCon-Change (for peak latency, t (18) = 0.430, p = 0.672; for peak amplitude, t (18) = 0.482, p = 0.636).

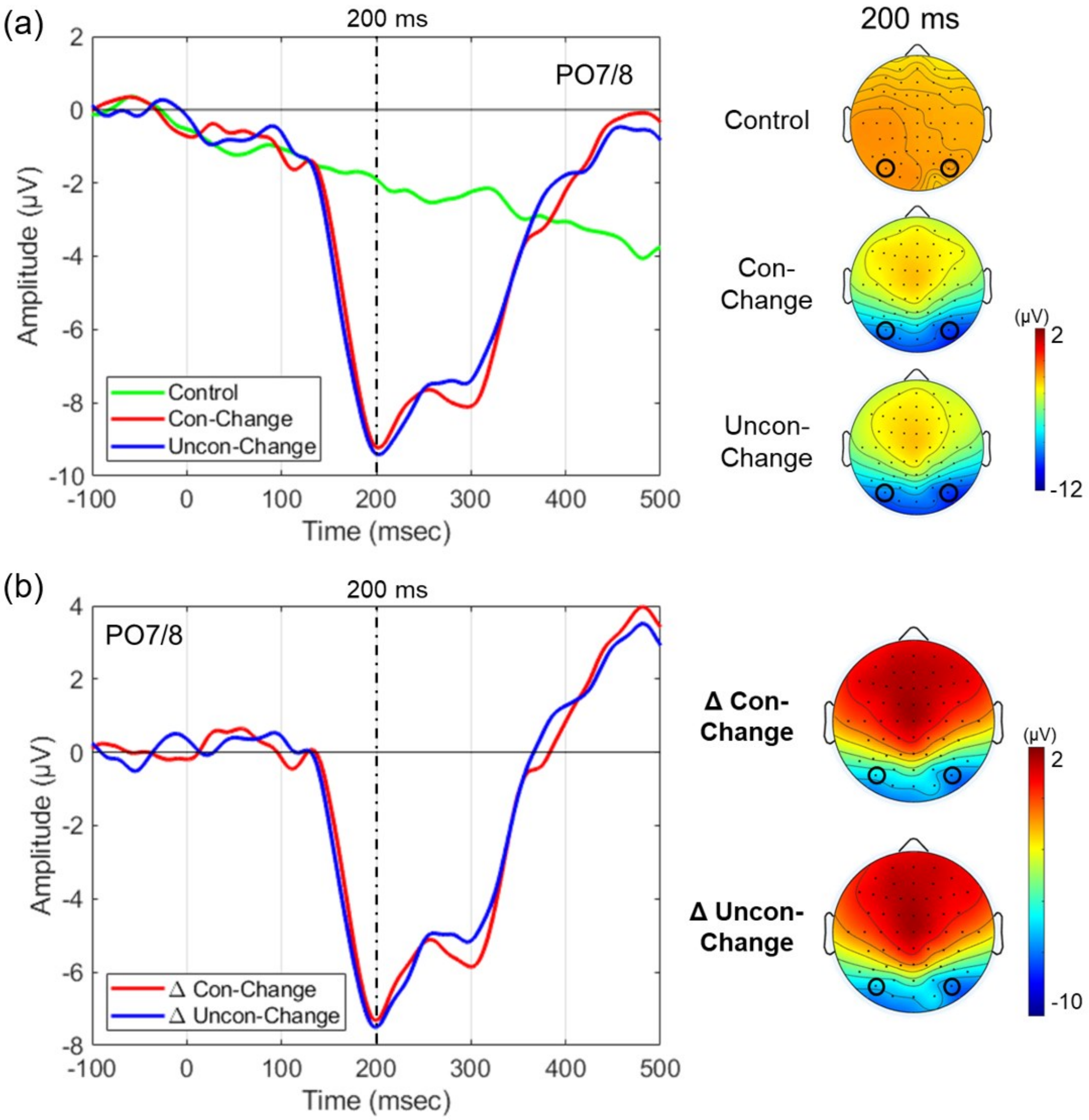

Figure 12. Grand-averaged VEPs for each condition and subtracted ones.

VEPs at PO7/8 and their isocontour maps at latencies of 200 ms were illustrated for each condition (a). Subtracted VEPs and their isocontour maps at latencies of 200 ms ware shown for the ΔCon-Change condition and ΔUncon-Change condition (b). Change-related N1 were observed at a latency range of approximately 200 ms.

5.2.3. Correlation between behavioral data and change-related N1

Figure 13 shows the results of correlation analyses for the change-related N1. In the ΔCon-Change, there was no significant relationship between the differential proportion of perceptual alternation and latency (ρ (19) = 0.035, p = 0.887) or amplitude (ρ (19) = 0.075, p = 0.759) across participants. As for the ΔUncon-Change, there was also no significant relationship between the differential proportion of perceptual alternation and latency (ρ (19) = 0.236, p = 0.330) or amplitude (ρ (19) = 0265, p = 0.272) across participants. These results indicate that the amplitude of change-related N1 is not correlated with the facilitation of perceptual alternation in binocular rivalry regardless of whether the change of the visual stimulus was presented consciously or unconsciously.

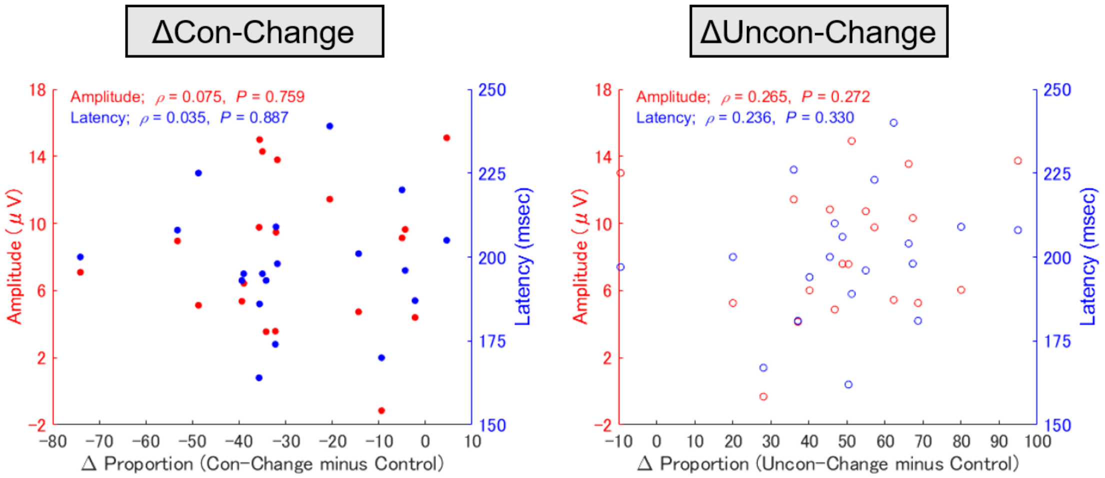

Figure 13. Relationship between proportion of perceptual alternation and change-related N1 across participants.

The correlations between the differential proportion of perceptual alternation and change-related N1 amplitude/latency are shown for each subtracted condition. There was no significant correlation for all conditions.

5.3. Discussion

In Experiment 3, to test the hypothesis that change-related N1 is relevant to APVA, we presented the abrupt change of the visual stimulus without temporal regularity to either of both eyes and investigated the correlation between the change-related N1 and the proportion of perceptual alternation in binocular rivalry. Consequently, we found no significant correlation between the enhancement of N1 amplitude and the facilitation of perceptual alternation when the change was presented consciously or unconsciously. These results indicated that the amplitude of change-related N1 is not relevant to the individual difference in APVA.

While no correlation was found between change-related N1 and the proportion of perceptual alternation, the behavioral results are consistent with Experiment 1 using mismatch stimuli in that perceptual alternation was promoted under the unconscious condition and suppressed under the conscious condition. These results suggest that the amplitude of change-related response is not related to the individual difference in APVA, although the sudden change stimulus is related to the facilitation of perceptual alternation when the visual stimulus was presented unconsciously. However, the final behavioral output through the neural information processing (e.g. the trend of change in perceptual alternation) would be the same for both the mismatch deviant and sudden change. Thus, vMMN and change-related responses may play different roles in APVA.

In summary, the results showed no correlation between the enhancement of change-related N1 and the facilitation of perceptual alternation in binocular rivalry regardless of whether the change of the visual stimulus was presented consciously or unconsciously. In addition, the proportion of perceptual alternation was promoted when the abrupt change of visual stimulus was presented unconsciously. These results imply that the change without temporal regularity is involved in APVA, but the magnitude of change-related responses may not be involved in promotion of APVA.

6. General discussion

We mainly discuss the following three points. First, we summarize the neural mechanism of APVA that we found from the experiments using mismatch stimuli in binocular rivalry (Experiments 1 and 2). Second, whether the vMMN-specific mechanism or the common mechanism between vMMN and change-related response is involved in the neural mechanism of APVA, comparing the experiment using mismatch stimuli with the experiment using change-related stimuli (Experiments 1 and 3). Finally, underlying the assumption that the common mechanism is involved in APVA, we consider neural representations that reflect this common mechanism.

The results in the experiments with a mismatch stimulus in binocular rivalry show following neural activities which reflect the neural mechanism of APVA. After the vMMN including promotive information of conscious perception in its amplitude is evoked at around 130 ms from the stimulus onset, the phase in the theta band activity at posterior areas tends to be coherent in the latency range of approximately 200–400 ms. Since VAN, which is one component of the earliest brain activities related to visual awareness, is observed at 200 ms, the phase coherence may be relevant to the last stage for visual awareness. These findings will shed light on the study of APVA as a first step.

In Experiment 1 and 3, The present study showed that the unconscious mismatch deviant as well as the unconscious unexpected change makes the unconscious stimulus more likely to be consciously perceived. However, regarding the correlation between these neural activity and behavior, vMMN amplitude correlated with the facilitation of perceptual alternation, but change-related N1 did not. In the predictive coding theory, the brain monitors the error between sensory input and an internal prediction model, and it takes actions to minimize the prediction error (Friston, 2005; Friston & Kiebel, 2009; Hohwy, 2012). The images of stimulus change are exactly the same in Experiments 1 and 3. However, in the experiment with a mismatch stimulus, the timing of stimulus presentation could be predicted by intermittent presentation of the stimulus, whereas in the experiment with a change-related stimulus, the timing of stimulus presentation could not be predicted because there was no clue. In other words, the precision of prediction models is higher for mismatch stimuli with the prior knowledge due to the temporal regularity than for change-related stimuli. The higher the precision of predictions for the target stimulus, the greater the gap between the predicted perception and the actual sensory input when an unexpected stimulus is presented. Therefore, the deviant stimulus has a larger prediction error with the internal model than the simple changing stimulus.

Active inference model based on predictive coding theory assumes that the brain corrects the prediction of perception in response to an unpredicted stimulus by preferentially adopting another prediction which differs from the current one and attempts to minimize prediction errors (Parr et al., 2019; Whyte and Smith, 2021). In binocular rivalry, the brain has predictions for two images input to the left and right eyes, and only one is adopted and perceived. According to active inference model, when an unexpected image is presented, the brain tries to reduce the prediction error by perceiving the other image that are different from the current one. Thus, the only way to minimize the prediction error is to perceive another image in binocular rivalry, that is, to cause perceptual alternation. Previous studies have also reported that the prior knowledge of stimulus prediction affects the perception of the next presented stimulus in binocular rivalry (Denison et al., 2011; Andermane et al., 2020). The above ideas apply to both stimulus changes in Experiment 1 and Experiment 3. However, since the mismatch stimulus has the larger prediction error, the interindividual differences may have been more pronounced in the vMMN than in the change-related N1. The difference in these correlations is considered to come from the difference in the intensity of prediction. Taken together, these results indicate that the neural mechanism common to vMMN and change-related N1, which the neural information processing underlying the prediction of the visual images, is an important factor in the neural mechanism of APVA.

If the prediction mechanism is involved in APVA, what kind of neural representation is it reflected? The present study showed that theta ITPC of vMORs tends to correlate with the facilitation of perceptual alternation when the deviant stimulus was presented unconsciously in Experiment 2. The enhancement of neural activity by the deviant mirrors an increase of prediction error (Friston, 2005; Stefanics et al., 2014). The increase in theta band ITPC evoked by the deviant is also considered to reflect the increase in prediction error as well as vMMN. Therefore, the enhancement of theta band ITPC in vMORs is a likely candidate for the neural representations reflecting the prediction mechanism. On the other hand, the network synchronization theory (NetSync) proposed that phase synchronization is necessary for the interaction between attention and phenomenal consciousness systems (Nani et al., 2019). According to NetSync, there are an attention system based on the fronto-parietal network and an unconscious network based on the temporo-parietal-occipital network, and conscious experience is formed by phase synchronization between these networks. This theory is consistent with our proposed idea that the phase coherence in posterior area associated with the mismatch process and the consequent enhancement of the attention system facilitate the conscious perception of the unconscious stimulus (the third paragraph in "4.3. Discussion" for detail). Taken together, It is highly likely that phase synchronization between the unconscious system based on the posterior regions and the attention system based on the frontal regions reflects the information processing that causes conscious perception of the unconscious visual stimulus. Therefore, we suggest that the theta band phase synchronization between frontal and posterior regions is involved in the neural mechanism of APVA. However, the current results show inter-trial phase coherence in the posterior site, which does not necessarily reflect phase synchronization between frontal and posterior regions. In the future, it will be necessary to separate the networks of the frontal and posterior regions and analyze their phase synchronization to experimentally verify our proposal.

In summary, the neural mechanism common to vMMN and change-related N1 appears to be involved in APVA. The common mechanism is considered to be a perceptual update function for prediction error minimization based on predictive coding theory. However, the contribution to APVA is more pronounced in vMMN than in change-related N1, and this difference may be attributed to the intensity of prediction error. Furthermore, we examined the effect of neural activity evoked by the unconscious deviant on conscious perception from the viewpoint of oscillatory responses. As a result, the theta band ITPC at the posterior site involved in the unconscious mismatch process promotes the conscious perception of the unconscious visual stimulus. This result indicates that the phase coherence associated with the mismatch process and the concomitant enhancement of the attention system facilitate the conscious perception of the unconscious stimulus. These results suggest that the theta band phase synchronization between frontal and posterior regions reflects the neural mechanism of APVA

7. Conclusion

To clarify the neural mechanism of APVA, we investigated the correlation between vMMN, vMOR, change-related N1 and the facilitation of perceptual alternation on binocular rivalry, respectively. Consequently, vMMN and vMORs were observed at the latency range of about 130 ms and approximately 200–400 ms, respectively. Both the amplitude of vMMN and theta band ITPC are related to the facilitation of perceptual alternation in binocular rivalry. These results indicate that neural processing reflected by an increase of vMMN amplitude followed by an increase in theta band ITPC is related to APVA. In behavior, the stimuli evoking either vMMN or change-related N1 made the unconscious stimulus easier to be consciously perceived. vMMN positively correlated with the individual differences in perceptual alternation, whereas change-related N1 did not. These results indicate that the neural mechanism common to vMMN and change-related N1 is involved in the neural mechanism of APVA, while difference in information processing of prediction affects individual differences in APVA. On the other hand, theta band ITPC of vMORs tended to correlate with the facilitation of perceptual alternation. These results may suggest the increase of theta band phase alignment induced by the mismatch process and the accompanying enhancement of the attentional system play important roles in the neural mechanism of APVA.

8. References

Alais D, Cass J, O'Shea RP, Blake R (2010) Visual sensitivity underlying changes in visual consciousness. Curr Biol 20:1362-1367.

Andermane N, Bosten JM, Seth AK, Ward J (2020) Individual differences in the tendency to see the expected. Conscious Cogn 85:102989.

Aru J, Bachmann T, Singer W, Melloni L (2012) Distilling the neural correlates of consciousness. Neurosci Biobehav Rev 36:737-746.

Ashmead, J (2010) Morlet wavelets in quantum mechanics. arXiv preprint arXiv 1001:0250.

Astikainen P, Lillstrang E, Ruusuvirta T (2008) Visual mismatch negativity for changes in orientation–a sensory memory-dependent response. Eur J Neurosci 28:2319-2324.

Bor D, Seth AK (2012) Consciousness and the prefrontal parietal network: Insights from attention, working memory, and chunking. Front Psychol 3:63.

Brainard DH (1997) The Psychophysics Toolbox. Spat Vis 10:433-436.

Chica AB, Lasaponara S, Lupiáñez J, Doricchi F, Bartolomeo P (2010) Exogenous attention can capture perceptual consciousness: ERP and behavioural evidence. Neuroimage 51:1205-1212.

Chica AB, Lasaponara S, Chanes L, Valero-Cabré A, Doricchi F, Lupiáñez J, Bartolomeo P (2011) Spatial attention and conscious perception: The role of endogenous and exogenous orienting. Atten Percept Psychophys 73:1065-1081.

Cohen MA, Cavanagh P, Chun MM, Nakayama K (2012) The attentional requirements of consciousness. Trends Cogn Sci 16:411-417.

Crick F, Koch C (1990) Towards a neurobiological theory of consciousness. Semin

Neurosci, pp 263-275: Saunders Scientific Publications.

Czigler I, Balázs L, Winkler I (2002) Memory-based detection of task-irrelevant visual changes. Psychophysiology 39:869-873.

Davidson MJ, Alais D, van Boxtel JJ, Tsuchiya N (2018) Attention periodically samples competing stimuli during binocular rivalry. Elife 7:e40868.

Dehaene S, Changeux J-P (2011) Experimental and theoretical approaches to conscious processing. Neuron 70:200-227.

Denison RN, Piazza EA, Silver MA (2011) Predictive context influences perceptual selection during binocular rivalry. Front Hum Neurosci 5:166.

Doniger GM, Foxe JJ, Schroeder CE, Murray MM, Higgins BA, Javitt DC (2001) Visual perceptual learning in human object recognition areas: A repetition priming study using high-density electrical mapping. Neuroimage 13:305-313.

Drew, A., Torralba, M., Ruzzoli, M., Fernández, L.M., Sabaté, A., Pápai, M.S., and Soto-Faraco, S. (2019). Neural evidence of cognitive conflict during binocular rivalry. *SSRN Journal*.
doi: 10.2139/ssrn.3501843

Eklund R, Wiens S (2018) Visual awareness negativity is an early neural correlate of awareness: A preregistered study with two Gabor sizes. Cogn Affect Behav Neurosci 18:176-188.

Friston K (2005) A theory of cortical responses. Philos Trans R Soc Lond B Biol Sci 360:815-836.

Friston K, Kiebel S (2009) Predictive coding under the free-energy principle. Philos Trans R Soc Lond B Biol Sci 364:1211-1221.

Frässle S, Sommer J, Jansen A, Naber M, Einhäuser W (2014) Binocular rivalry:

Frontal activity relates to introspection and action but not to perception. J Neurosci 34:1738-1747.

Förster J, Koivisto M, Revonsuo A (2020) ERP and MEG correlates of visual consciousness: The second decade. Conscious Cogn 80:102917.

Giller F, Bensmann W, Mückschel M, Stock AK, Beste C (2020) Evidence for a causal role of superior frontal cortex theta oscillations during the processing of joint subliminal and conscious conflicts. Cortex 132:15-28.

Grandchamp R, Delorme A (2011) Single-trial normalization for event-related spectral decomposition reduces sensitivity to noisy trials. Front Psychol 2:236.

Guthrie D, Buchwald JS (1991) Significance testing of difference potentials. Psychophysiology 28:240-244.

Haque H, Lobier M, Palva JM, Palva S (2020) Neuronal correlates of full and partial visual conscious perception. Conscious Cogn 78:102863.

Hedge C, Stothart G, Todd Jones J, Rojas Frías P, Magee KL, Brooks JC (2015) A frontal attention mechanism in the visual mismatch negativity. Behav Brain Res 293:173-181.

Hohwy J (2012) Attention and conscious perception in the hypothesis testing brain. Front Psychol 3:96.

Jack BN, Widmann A, O'Shea RP, Schröger E, Roeber U (2017) Brain activity from stimuli that are not perceived: Visual mismatch negativity during binocular rivalry suppression. Psychophysiology 54:755-763.

Jiang Y, Costello P, Fang F, Huang M, He S (2006) A gender- and sexual orientation-dependent spatial attentional effect of invisible images. Proc Natl Acad Sci USA 103:17048-17052.

Kanai R, Moradi F, Shimojo S, Verstraten FA (2005) Perceptual alternation induced by visual transients. Perception 34:803-822.

Kimura M, Katayama Ji, Ohira H, Schröger E (2009) Visual mismatch negativity: New evidence from the equiprobable paradigm. Psychophysiology 46:402-409.

Kimura M (2012) Visual mismatch negativity and unintentional temporal-context-based prediction in vision. Int J Psychophysiol 83:144-155.

Koch C, Massimini M, Boly M, Tononi G (2016) Neural correlates of consciousness: progress and problems. Nat Rev Neurosci 17:307-321.

Koivisto M, Revonsuo A (2003) An ERP study of change detection, change blindness, and visual awareness. Psychophysiology 40:423-429.

Koivisto M, Kainulainen P, Revonsuo A (2009) The relationship between awareness and attention: Evidence from ERP responses. Neuropsychologia 47:2891-2899.

Koivisto M, Revonsuo A (2010) Event-related brain potential correlates of visual awareness. Neurosci Biobehav Rev 34:922-934.

Koivisto M, Grassini S (2016) Neural processing around 200 ms after stimulus-onset correlates with subjective visual awareness. Neuropsychologia 84:235-243.

Koivisto M, Grassini S, Salminen-Vaparanta N, Revonsuo A (2017) Different electrophysiological correlates of visual awareness for detection and identification. J Cogn Neurosci 29:1621-1631.

Kurita Y, Urakawa T, Araki O (2021) Involvement of visual mismatch negativity in access processing to visual awareness. Front Hum Neurosci 15:757411.

Kurita Y, Urakawa T, Araki O (2023) Theta phase coherence in visual mismatch responses involved in access processing to visual awareness. Front Hum Neurosci, Accepted.

Lee SH, Blake R, Heeger DJ (2005) Traveling waves of activity in primary visual cortex during binocular rivalry. Nat Neurosci 8:22-23.

Lumer ED, Friston KJ, Rees G (1998) Neural correlates of perceptual rivalry in the human brain. Science 280:1930-1934.

MacLean SE, Ward LM (2014) Temporo-frontal phase synchronization supports hierarchical network for mismatch negativity. Clin Neurophysiol 125:1604-1617.

Maekawa T, Goto Y, Kinukawa N, Taniwaki T, Kanba S, Tobimatsu S (2005) Functional characterization of mismatch negativity to a visual stimulus. Clinical neurophysiology 116:2392-2402.

Makeig S (1993) Auditory event-related dynamics of the EEG spectrum and effects of exposure to tones. Electroencephalogr Clin Neurophysiol 86(4):283-293.

Nani A, Manuello J, Mancuso L, Liloia D, Costa T, Cauda F (2019) The neural correlates of consciousness and attention: Two sister rocesses of the brain. Front Neurosci 13:1169.

Paffen CL, Van der Stigchel S (2010) Shifting spatial attention makes you flip: Exogenous visual attention triggers perceptual alternations during binocular rivalry. Atten Percept Psychophys 72:1237-1243.

Paffen CL, Alais D (2011) Attentional modulation of binocular rivalry. Front Hum Neurosci 5:105.

Parr T, Corcoran AW, Friston KJ, Hohwy J (2019) Perceptual awareness and active inference. Neurosci Conscious 2019:niz012.

Pelli DG (1997) The VideoToolbox software for visual psychophysics: Transforming numbers into movies. Spat Vis 10:437-442.

Pitts MA, Metzler S, Hillyard SA (2014) Isolating neural correlates of conscious perception from neural correlates of reporting one's perception. Front Psychol 5:1078.

Polonsky A, Blake R, Braun J, Heeger DJ (2000) Neuronal activity in human primary visual cortex correlates with perception during binocular rivalry. Nat Neurosci 3:1153-1159.

Prinz J (2011) Is attention necessary and sufficient for consciousness. Attention: Philosophical and psychological essays:174-203.

Roeber U, Widmann A, Trujillo-Barreto NJ, Herrmann CS, O'Shea RP, Schröger E (2008) Early correlates of visual awareness in the human brain: Time and place from event-related brain potentials. J Vis 8:21.21-12.

Roeber U, Veser S, Schröger E, O'Shea RP (2011) On the role of attention in binocular rivalry: Electrophysiological evidence. PLoS One 6:e22612.

Salti M, Harel A, Marti S (2019) Conscious perception: Time for an update? J Cogn Neurosci 31:1-7.

Silverstein BH, Snodgrass M, Shevrin H, Kushwaha R (2015) P3b, consciousness, and complex unconscious processing. Cortex 73:216-227.

Stefanics G, Kremláček J, Czigler I (2014) Visual mismatch negativity: A predictive coding view. Front Hum Neurosci 8:666.

Stothart G, Kazanina N (2013) Oscillatory characteristics of the visual mismatch negativity: What evoked potentials aren't telling us. Front Hum Neurosci 7:426.

Tallon-Baudry C, Bertrand O, Delpuech C, Pernier J (1996) Stimulus specificity of phase-locked and non-phase-locked 40 Hz visual responses in human. J Neurosci 16(13): 4240-4249.

Torrence C, Compo GP (1998) A practical guide to wavelet analysis. Bulletin of the American Meteorological Society 79:61-78.

Urakawa T, Inui K, Yamashiro K, Kakigi R (2010) Cortical dynamics of the visual change detection process. Psychophysiology 47:905-912.

Urakawa T, Bunya M, Araki O (2017a) Involvement of the visual change detection process in facilitating perceptual alternation in the bistable image. Cogn Neurodyn 11:307-318.

Urakawa T, Aragaki T, Araki O (2017b) Exogenously-driven perceptual alternation of a bistable image: From the perspective of the visual change detection process. Neurosci Lett 653:92-96.

Urakawa T, Nagano K, Matsumoto Y, Araki O (2018) Enhancement of a genuine visual mismatch negativity correlates with the facilitation of perceptual alternation of a bistable image. Neuroreport 29:1104-1108.

Van Diepen RM, Mazaheri A (2018) The caveats of observing inter-trial phase-coherence in cognitive neuroscience. Sci Rep 8: 2990.

Veser S, O'Shea RP, Schröger E, Trujillo-Barreto NJ, Roeber U (2008) Early correlates of visual awareness following orientation and colour rivalry. Vision Res 48:2359-2369.

Vogel EK, Awh E (2008) How to exploit diversity for scientific gain: Using individual differences to constrain cognitive theory. Curr Dir Psychol Sci 17:171-176.

Walker P, Powell DJ (1979) The sensitivity of binocular rivalry to changes in the nondominant stimulus. Vision Res 19:247-249.

Whyte CJ, Smith R (2021) The predictive global neuronal workspace: A formal active inference model of visual consciousness. Prog Neurobiol 199:101918.

Winkler I, Czigler I (2012) Evidence from auditory and visual event-related potential (ERP) studies of deviance detection (MMN and vMMN) linking predictive coding theories and perceptual object representations. Int J Psychophysiol 83:132-143.

Wolfe JM (1983) Influence of spatial frequency, luminance, and duration on binocular rivalry and abnormal fusion of briefly presented dichoptic stimuli. Perception 12:447-456.

Yan T, Feng Y, Liu T, Wang L, Mu N, Dong X, Liu Z, Qin T, Tang X, Zhao L (2017) Theta oscillations related to orientation recognition in unattended condition: A vMMN study. Front Behav Neurosci 11:166.

開一夫, 金山範明 (2020) 脳波解析入門 Windows10対応版. 東京大学出版会. p.125-155.

Glossary

- ANOVA (analysis of variance):

  A statistical test for significant differences in the means of three or more groups.

- APVA (access processing to visual awareness):

  A type of the unconscious neural processing that determines whether the unconscious stimulus is consciously perceived or not.

- EEG (electroencephalography, or electroencephalogram):

  The electrical activity recorded by electrodes placed on the scalp or elsewhere. Electroencephalogram generally refers to the electrical activity, and the technique for recording it is called electroencephalography. Both are abbreviated as EEG.

- EOG (electrooculogram):

  A method to measure potential fluctuations associated with eye movement from electrodes attached around the orbit (typically electrodes placed above and below the eyes).

- ERSP (event-related spectral perturbation):

  Sum of the squared oscillation amplitudes. An enhancement of ERSP corresponds to an increase in the neural information processing.

- fMRI (functional magnetic resonance imaging):

  A technique in which brain activities are imaged and measured as signal changes associated with brain functional activity. In general, fMRI has higher spatial resolution than EEG.

- ISI (inter-stimulus interval):

  The time range from the stimulus offset to the next stimulus onset.

- ITI (inter-trial interval):

Time span from the end of one trial to the start of the next trial.

- ITPC (inter-trial phase coherence):

  Mean phase in EEG waves over trials. ITPC from 0 to 1 represents the degree of the phase coherence in trials.

- NCC (neural correlate of consciousness):

  The minimal set of neuronal events or mechanisms sufficient for a specific conscious perception.

- N1 (also called N100):

  One component of the most basic evoked potentials by a visual stimulus. The negative peak observed in occipital region at about 130–200 ms after the onset of visual stimulus.

- P1 (also called P100):

  One component of the most basic evoked potentials by a visual stimulus. The positive peak observed in occipital region at about 100 ms after the onset of visual stimulus.

- vMMN (visual mismatch negativity):

  One component of the visual evoked potential. VMMN is a negative-going enhancement over posterior electrodes at a latency of approximately 130–250 ms when comparing responses to an infrequently presented visual stimulus (deviant) and a repetitively presented stimulus (standard). VMMN reflects automatic visual change detection based on temporal regularity.

- vMOR (visual mismatch oscillatory response):

  Oscillatory responses associated with visual mismatch process. VMOR is an enhancement of the oscillatory responses (typically, the theta band (4–8 Hz) is enhanced) over posterior electrodes at a latency of approximately 100–350 ms when responses to an infrequently presented visual stimulus (deviant) and a repetitively presented stimulus (standard).

- VAN (visual awareness negativity):

  One component of the earliest visual evoked potential related to visual awareness. VAN is observed in posterior region at a latency of about 200 ms after the onset of visual stimulus.

- VEP (visual evoked potential):

  An evoked potential caused by a visual event.

- Oz, PO3, PO4, PO7, PO8:

  Position of electrodes on the scalp as defined by the international 10–20 system. The layout of the electrodes in this study are shown in Figure 14 below.

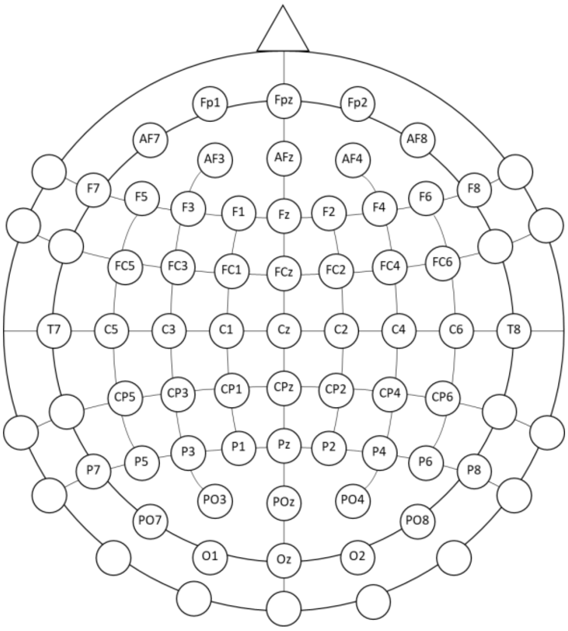

Figure 14. The layout of the electrodes.

The positions of the electrodes used in this study are shown. The layout of the electrodes is modified based on the international 10–20 system.